





Research Article

Tracking Late Holocene climate change and the 1908 Tunguska impact event from lake sediments in Central Siberia

D.Y. Rogozin^{a,b} , L.B. Nazarova^{c,d}, N.A. Rudaya^{e,f}, L.A. Frolova^{c,e} , G.N. Bolobanshchikova^a, O.V. Palagushkina^c , A.V. Darin^g  and A.V. Meydus^h

^aInstitute of Biophysics, Siberian Branch of Russian Academy of Sciences, Akademgorodok 50-50, 660036, Krasnoyarsk, Russia; ^bSiberian Federal University, 79 Svobodnyi Ave., Krasnoyarsk 660041, Russia; ^cKazan Federal University, 18 Kremlyovskaya str., 420008 Kazan, Russia; ^dAlfred Wegener Institute, Helmholtz Center for Polar and Marine Research, Research Unit Potsdam, Telegrafenberg A43, 14473 Potsdam, Germany; ^eInstitute of Archaeology & Ethnography, Russian Academy of Sciences, Siberian Branch, 17 Lavrentieva Ave., 630090, Novosibirsk, Russia; ^fBiological Institute, Tomsk State University, 36 Lenina str., 634050, Tomsk, Russia; ^gInstitute of Geology and Mineralogy Siberian Branch of Russian Academy of Sciences, 3 Prospekt Koptyuga, 630090, Novosibirsk, Russia and ^hAstafiev Krasnoyarsk State Pedagogical University, 89 Ady Lebedevoi, 660049, Krasnoyarsk, Russia

Abstract

We studied a 2200-year-old sediment core from Lake Zapovednoye, a small, deep, freshwater lake near the site of the 1908 Tunguska impact event. Analysis of the sediment core for geochemistry, pollen, chironomids, Cladocera, and diatoms revealed traces of climatic fluctuations during the investigated time period during which a cool climate before 1000 CE was replaced by the Medieval Climatic Optimum, the Little Ice Age, and finally the modern warming. An increased content of terrigenous elements was identified at the depth corresponding to ca. 1908 CE. This layer presumably resulted from erosion of the soil cover after the tree fall caused by the Tunguska impact event (the largest recorded in history). For the first time, the reaction of lake biota to an impact event has been detected. Our study has demonstrated that the taxonomic diversity of hydrobionts (chironomids and cladocerans) significantly declined after the catastrophe, probably due to increased turbidity, and recovered in 6–10 years. The pollen and diatom assemblages, however, demonstrated weaker compositional shifts.

Keywords: Climate change, Siberia, 1908 Tunguska impact event, XRF, permafrost, pollen, chironomids, Cladocera, diatoms

INTRODUCTION

Many recent studies considering the impact of climate change within the circumpolar North have confirmed its polar amplification, so even small climatic fluctuations cause more significant changes in the northern regions than in other parts of the world (Pörtner et al., 2022). This is due to the positive feedback associated with sea ice and snow cover, anthropogenic pollution of the Arctic environment, and an increase in cloud cover and water vapor (Kirtman et al., 2013). Under modern global warming, these effects can lead to significant changes in ecosystems, and the forecast of these changes is especially relevant for the Arctic and adjacent regions (Self et al., 2015). In turn, to justify these forecasts, one needs information on climate-induced changes that occurred in the past.

The part of Central Siberia locked between the Yenisei River and the western border of the Republic of Sakha (Yakutia) that includes Evenkia (Evenki District of Krasnoyarsk Krai, Russia) is currently much less explored than the neighboring regions of Siberia, the main reason being the inaccessibility of this region and its remoteness from more developed areas.

Corresponding author: D.Y. Rogozin; Email: rogozin@ibp.ru

Cite this article: Rogozin DY, Nazarova LB, Rudaya NA, Frolova LA, Bolobanshchikova GN, Palagushkina OV, Darin AV, Meydus AV (2025). Tracking Late Holocene climate change and the 1908 Tunguska impact event from lake sediments in Central Siberia. *Quaternary Research* 1–19. <https://doi.org/10.1017/qua.2024.35>

The Central Tunguska Plateau, located in the middle of the Central Siberia Plateau, is almost unexplored in terms of its paleoenvironment (Fig. 1). The paleolimnological reconstructions of the Holocene in Siberia published so far have been based on data collected from the neighboring territories that belong to other climatic zones (i.e., Blyakharchuk et al., 2007; Müller et al., 2009; Fedotov et al., 2012, 2013; Krivonogov et al., 2012, 2023; Rudaya et al., 2012, 2016, 2020; Nazarova et al., 2013; Frolova et al., 2017; Subetto et al., 2017; Zhilich et al., 2017; Wetterich et al., 2018; Glückler et al., 2022; Kobe et al., 2022; Karachurina et al., 2023, etc.). Of the lakes that have been investigated so far, the closest in terms of distance and climatic conditions is Lake Khamra (Khamra), located 600 km to the east in Yakutia (Baisheva et al., 2024) (Fig. 1).

The Evenkia region is interesting not only because it is poorly studied compared to neighboring territories, but also because the influence of moisture transfer from both the Atlantic and Pacific oceans is weaker here than in neighboring regions of Siberia (Vasiliev et al., 2003). Additionally, the Central Tunguska Plateau is located at the border of the permafrost zone, which, in view of global warming, is of particular interest (Palagushkina et al., 2017; Biskaborn et al., 2019; Wetterich et al., 2021).

This territory is also known worldwide for the so-called 1908 Tunguska impact event (herein Tunguska event or Event), which occurred here on June 30, 1908. The Event was a unique, powerful atmospheric explosion of unknown nature, its estimated epicenter located at 60°54′11″N and 101°54′35″E (Farinella et al., 2001;

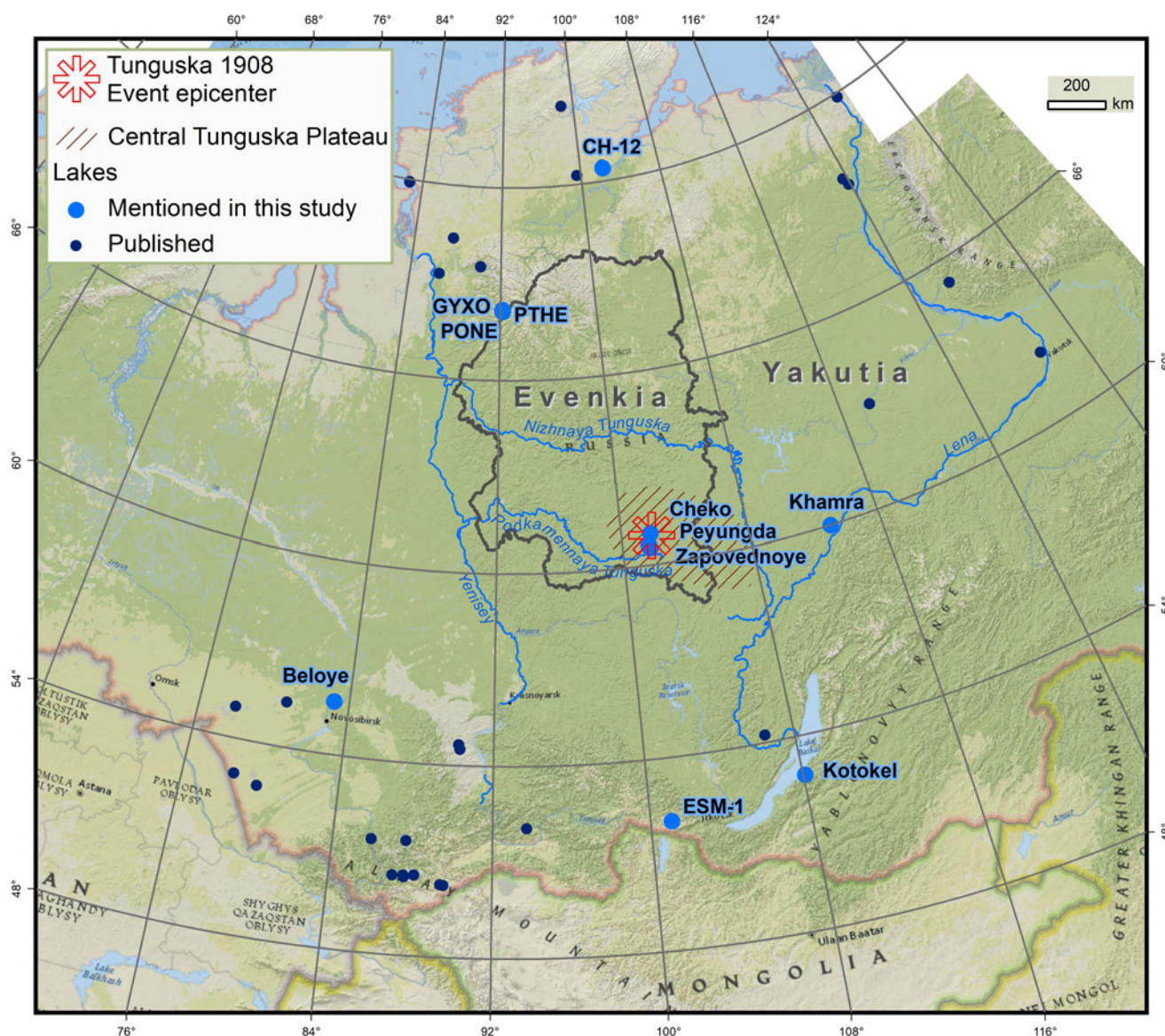


Figure 1. Overview map of published paleolimnological studies in Central Siberia.

Jenniskens, 2019; Gladysheva, 2020), that remains the most significant impact in the Earth's recorded history, though much larger impacts occurred in prehistoric times (Longo, 2007). The explosion over the sparsely populated east Siberian taiga flattened over 80 million trees over an area of 2200 km² and was registered at seismic stations across Eurasia. The air waves from the blast were detected as far away as Jakarta, Indonesia (then known as Batavia, Dutch East Indies), and Washington, DC (Whipple, 1934). The Event is generally attributed to the atmospheric explosion of a stony asteroid about 50–60 m in size (Longo et al., 1994; Hou et al., 1998, 2004; Kolesnikov et al., 1999, 2003; Morrison, 2018), but several other scenarios have been proposed to explain it (Longo, 2007; Khrennikov et al., 2020).

The possible impact of the Event on the surrounding ecosystems is still poorly studied, and nearly no data are available about the influence it had on the aquatic ecosystems situated in close proximity to the explosion. Until now, no clear traces of the Event have been found in lake sediments (Rogozin et al., 2017).

We investigated Lake Zapovednoye, a small deep lake of unknown origin situated about 70 km to the south of the Tunguska event epicenter (Vasiliev et al., 2003; Gladysheva, 2020). The main aim of our study was to reconstruct the paleoclimate and paleoenvironment of the Central Tunguska Plateau (Central Siberia), one of the least-studied regions of Eurasia, using a multiproxy approach that considers the data accumulated on the geochemistry, pollen, chironomids, Cladocera, and diatoms of the lake. Special attention was given to possible traces of the Tunguska event, since their identification in the bottom sediments could increase our knowledge about this still incomprehensible phenomenon and support the dating of the upper layers of the studied sediment core.

Study area

The Central Tunguska Plateau is a relatively low tuffogenic volcanic mountain area in Central Siberia, Russia, and is a part of the Central Siberian Plateau situated between the Yenisei and Lena

ivers (Vasiliev et al., 2003; Fig. 1). Deeply incised river valleys dissect the plateau. The average elevations are 200–300 meters above sea level (m asl), and maximum heights are slightly over 500 m asl (Vasiliev et al., 2003).

The climate of the region is sharply continental with large amplitudes in daily and seasonal temperatures. The annual precipitation is 380–420 mm, the maximum reached in July–August. The mean annual air temperature is -6°C . The mean July temperature is $+17^{\circ}\text{C}$; however, it often rises above $+30^{\circ}\text{C}$ during the warmest month. The average January temperature is -30°C and can drop to -55 or even -59°C . In summer, a low-pressure zone with weak winds prevails here (Vasiliev and Lvov, 2003). The rivers are fed mainly by snow (70% of the annual runoff) (Vasiliev et al., 2003).

The Central Tunguska Plateau is located at the southern border of the permafrost distribution zone and is characterized by active cryogenic processes: accumulation and degradation of permafrost (Vasiliev et al., 2003). The permafrost boundary runs along the Podkamennaya Tunguska River. Vegetation in this area occupies an intermediate position between the pine southern taiga and northern larch taiga forests. Mixed *Larix–Pinus* and *Betula–Pinus–Larix* forests with a well-defined shrub layer and a weakly expressed grass cover prevail (Shumilova, 1962; Vasiliev et al., 2003).

Lake Zapovednoye

Lake Zapovednoye ($60^{\circ}31.685'\text{N}$, $101^{\circ}43.710'\text{E}$) is located on the Central Tunguska Plateau, 60 km northwest of the nearest settlement, the village of Vanavara, and approximately 70 km south of the estimated epicenter of the Tunguska event. The lake is part of the small Verkhnyaya Lakura River basin, a tributary of a larger

river, Podkamennaya Tunguska, which flows into the Yenisei River (Fig. 1).

The lake is almost round and about 500 m in diameter. The maximum depth is 60.3 m at $60^{\circ}31.688'\text{N}$, $101^{\circ}43.740'\text{E}$, located near the geometric center of the lake, slightly closer to the eastern shore. The lake bottom is shaped like a regular conical funnel and has a shallow littoral zone. Seismoacoustic studies of the bottom showed that the thickness of the lake sediments is about 4 m, with hard rocks lying below (Rogozin et al., 2023). The Verkhnyaya Lakura River flows into the lake at its northwestern corner and flows out of the lake in the south (Fig. 2). There is no information regarding the origin of the lake.

METHODS

Sampling

A sediment core of 124 cm in length was retrieved on March 23, 2015, from the deepest part of the lake (Fig. 2; $60^{\circ}31.699'\text{N}$, $101^{\circ}43.648'\text{E}$). The core was taken from the ice surface, using a UWITEC gravity sampler (Austria) and removable plastic tubes of 90 mm in diameter. A transparent tube was used for visual control of the sediments. The sediment–water interface of the core was clearly visible and did not indicate loss or destruction of the upper sediment layers.

The core was split in half lengthwise. One half was cut into 1 cm samples. The samples were placed in sealed polyethylene bags, stored in darkness at -20°C , and used for ^{14}C , ^{210}Pb , and ^{137}Cs dating and proxy analyses. The other half was used to prepare solid blocks for X-ray fluorescence (XRF) element analysis. To do so, $170 \times 15 \times 6$ mm sediment blocks were extracted from the wet half core, freeze-dried, impregnated with epoxy resin, and polished following Boës and Fagel (2005).

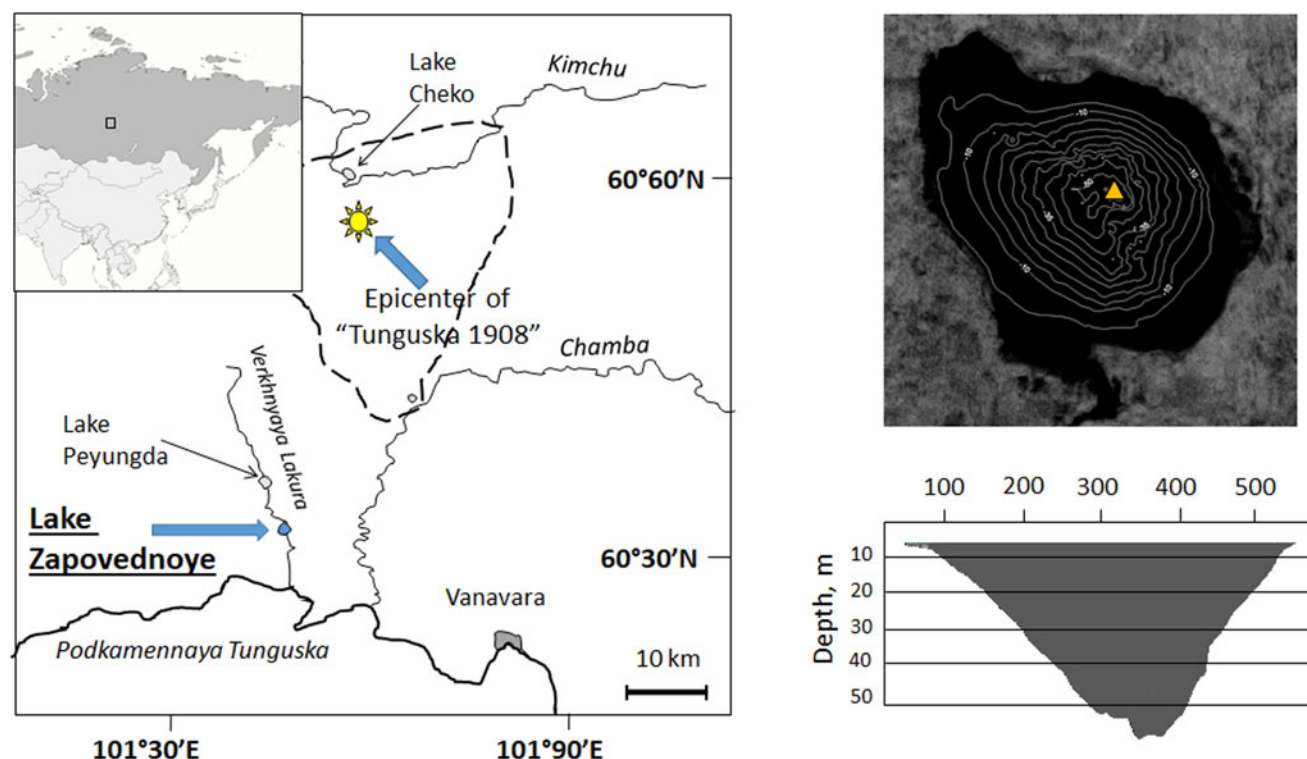


Figure 2. Geographic position and morphological characteristics of Lake Zapovednoye. The dashed line indicates the estimated boundary of the 1908 Tunguska fire with the triangle to mark its core.

Detection of chironomids, Cladocera, pollen, and spores was performed at a 5 cm resolution between 0 and 10 cm, then at a 1 cm resolution in the layers that were presumed to correspond to the Tunguska event (10 to 17 cm), and then at a 10 cm resolution between 17 and 124 cm. Diatom analysis was done at a 1 cm resolution over the entire depth of the sediments. Water content was determined in subsamples every 1 cm, and loss-on-ignition at 550°C (LOI₅₅₀) was determined in subsamples every 5 cm.

Dating

Twenty-three uppermost sediment samples (1 cm thick) were taken for ¹³⁷Cs, ²¹⁰Pb, and ²²⁶Ra measurements. The activity of ¹³⁷Cs, ²¹⁰Pb, and ²²⁶Ra was measured using previously described methods (Gavshin et al., 2004) of semiconductor low-background gamma spectrometry, on a coaxial Ge detector with a low-background cryostat EGPC-192-P21 connected to a spectrometer with a FP-6300B processor (EURISYS MESURES).

The modern sedimentation rate was estimated based on an assumption that the ¹³⁷Cs maximum in the lake sediments marks the global fallout after nuclear tests at the Novaya Zemlya site in 1961 (Krishnaswami and Lal, 1978). The ²²⁶Ra activity values were subtracted from the ²¹⁰Pb activity values to obtain the atmospheric ²¹⁰Pb (²¹⁰Pb_{ex}) according to generally accepted methods (Melgunov et al., 2003).

Two samples were taken from the core for the ¹⁴C dating. Radiocarbon analysis of bulk organic matter was carried out by the accelerator mass spectrometry (AMS) method in the NTUAMS laboratory of the National Taiwan University. The procedure for AMS ¹⁴C dating in the NTUAMS lab is described in Li et al. (2022). The program OxCal 4.4 was used for radiocarbon age analyses. The measured ¹⁴C ages were calibrated with the IntCal 20 curve (Reimer et al., 2020) (Table 1).

Elemental composition

Elemental composition was measured in the solid blocks at a resolution of 0.02 to 0.1 mm by applying synchrotron radiation micro-XRF analysis (XRF-SR) at the Institute of Nuclear Physics (Novosibirsk, Russia). The sediments in the lowest 10 cm were poorly preserved and excluded from the XRF analysis; thus, elemental analysis was performed at depths from 0 to 113 cm.

Pollen

The laboratory treatment for pollen analysis was carried out according to standard methods (Faegri and Iversen, 1989). One tablet of *Lycopodium* marker spores (batch 483216) was added to each sample for calculating the total pollen and spore concentrations as per Stockmarr (1971).

Counting was performed with a Zeiss AxioImager D2 light microscope at 400× magnification. Keys and atlases were used to determine the taxonomic identification of pollen and spores

(Kupriyanova and Alyoshina, 1978; Moore et al., 1991). Each sample contained a minimum of 300 pollen grains and spores. The spore–pollen diagram was produced in the TILIA software; zoning was performed after cluster analysis in the CONISS software (Grimm, 2004).

Chironomids

Treatment of sediment samples for chironomid analysis followed standard techniques described in Brooks et al. (2007). At least 50 head capsules were extracted from each sample to ascertain the diversity of the chironomid populations, sufficient for accurate estimation of the inferred temperature (Heiri and Lotter 2001; Quinlan and Smol, 2001). Chironomids were identified to the highest taxonomic resolution possible with reference to Wiederholm (1983) and Brooks et al. (2007). Information on the ecology of the chironomid taxa was taken from Brooks et al. (2007), Moller-Pilot (2009, 2013), and Nazarova et al. (2008, 2017, 2023). Percentage stratigraphic diagrams were built in C2 version 1.7.7 (Juggins, 2007). Zonation of the stratigraphy was accomplished using the optimal sum-of-squares partitioning method (Birks and Gordon, 1985) in the ZONE program (Lotter and Juggins, 1991). The number of significant zones was assessed using the broken stick model (Bennett, 1996) in the BSTICK program (Birks and Line, unpublished).

Cladocera

To analyze the subfossil chitinous remains of Cladocera from the bottom sediments of Lake Zapovednoye, we used the technique described by Korhola and Rautio (2001). Subsamples of dry sediments were deflocculated in 10% KOH and heated to 75°C for 30 minutes. The suspended matter was then rinsed through a 50 µm sieve. All samples were treated with ethanol to prevent decay, stained with safranin, and examined under an AxioLab A1 light microscope at 100–400× magnification. The remains were identified using specialized keys for both subfossil (Szeroczyńska and Sarmaja-Korjonen, 2007; Frolova, 2012) and modern Cladocera (Smirnov, 1971; Flößner, 2000; Kotov et al., 2010). A total of 4899 Cladocera remains were found. In each sample, between 217 and 437 chitinized remains of Cladocera were detected, of which 112 to 310 specimens per sample were identified. The number of specimens was calculated by using the largest number of parts of the organisms. The stratigraphic diagram was built in the TILIA program; zoning was performed using cluster analysis in the CONISS application (Grimm, 2004).

Diatoms

Samples of the investigated bottom sediments were dried for 24 hours at a temperature of 70°C. An aliquot of approximately 0.05 g was taken from each sample. Processing for diatom analysis followed the modified water bath method (Battarbee, 1986). The samples were treated with a 30% hydrogen peroxide solution by heating on a solid-state thermostat at a temperature of 90°C for 4 hours and constantly adding peroxide (Bolobanshchikova et al., 2015). After cooling, the samples were washed from peroxide by centrifugation in distilled water and diluted with distilled water to a final volume of 1.5 mL. Permanent slides were prepared using the Naphrax high refractive index resin. Diatoms were counted along parallel transects of up to 300 valves per sample using light microscopy (AxioScope 40, Zeiss) with immersion

Table 1. Radiocarbon dates from the Lake Zapovednoye bottom sediments.

Depth, cm	Lab code	¹⁴ C yr BP	cal yr BP
56–57	NTUAMS-4057	1150 ± 13	1045 ± 30
111–112	NTUAMS-4058	2099 ± 26	2075 ± 45

oil. Diatoms were identified as per Krammer and Lange-Bertalot (1986, 1988, 1991) and confirmed with modern taxonomy as given in the AlgaeBase database (Guiry and Guiry, 2023).

Numerical methods and mean July air temperature reconstruction

Effective occurrence numbers for biological communities were estimated using the N2 index (Hill, 1973). Principal Component Analysis (PCA) was used to explore the elemental core composition and main taxonomic variation patterns to compare the patterns against the hydrobiological data accumulated throughout the core (ter Braak and Prentice, 1988). Cluster analysis was performed in the PAST software (Hammer et al., 2001).

The quantitative reconstruction of the mean July air temperatures (T July) was performed using the North Russian (NR) chironomid-based temperature inference model (weighted averaging partial least squares [WA-PLS], two component; $r^2_{boot} = 0.81$; root mean square error of prediction [RMSEP] $boot = 1.43^\circ\text{C}$) based on a modern calibration data set of 193 lakes and 162 taxa from northern Russia (61–75°N, 50–140°E, T July range 1.8–18.8° C) (Nazarova et al., 2015). Mean July air temperature for the lakes in the calibration data set was derived from New et al. (2002). The T July NR model had been previously applied for paleoclimatic inferences in Siberia and northern Eurasia and has demonstrated the high reliability of the reconstructed parameters (Meyer et al., 2015; Plikt et al., 2019; Nazarova et al., 2020).

The chironomid-inferred T July were corrected to 0 m asl using a modern July air temperature lapse rate of $6^\circ\text{C}/\text{km}$ (Livingstone et al., 1999; Renssen et al., 2009; Heiri et al., 2014). According to New et al. (2002), mean July air temperature at the sampling site was 16.1°C . Taking into account the altitude of the lake at 329 m asl, the reconstructed T July was corrected by adding 1.97°C to the reconstructed values. Chironomid-based reconstructions were performed in C2 version 1.5 (Juggins, 2007). The chironomid data were square-root transformed to minimize species variance.

To assess the reliability of the chironomid-inferred T July reconstruction, we calculated the abundances of the rare (Hill's $N2 < 5$) or absent fossil chironomids in the modern calibration data set. To assess how similar the fossil samples were in respect to the temperature-based training data set, we used the goodness-of-fit (GoF) statistic derived from a canonical correspondence analysis (CCA) of the modern calibration data with the passively fitted fossil samples, using T July as the sole constraining variable (Birks et al., 1990).

Optima of the taxa that were rare in the modern data set were likely to be unreliably estimated (Brooks and Birks, 2001). To assess how unusual the fossil assemblages were with respect to the training set samples along the temperature gradient, we used the GoF statistics derived from a CCA of the modern calibration data and down-core passive samples with T July as the sole constraining variable (Birks et al., 1990). Fossil samples with a residual distance to the first CCA axis larger than the 90th and 95th percentile of the residual distances of all the modern samples were identified as samples with a “poor fit” and a “very poor fit” with the reconstructed variable (T July) (Birks et al., 1990).

PCA and CCA were performed using CANOCO 4.5 (ter Braak and Šmilauer, 2002). Chironomid percentage data were square-root transformed and rare taxa were downweighted. PCA for XRF elemental composition was performed in the R software environment (<https://www.r-project.org>; R Development Core Team, 2018). XRF

data were previously ($\log+1$) transformed. Zonation was carried out using cluster analysis and confirmed by PCA.

RESULTS AND INTERPRETATIONS

Core lithology and chronology

The sediments of Lake Zapovednoye consist of dark brown and black ferruginous clay with a high content of water and organic matter and have a layered structure. Below 107 cm the sediments became more compact with more-pronounced layering. The vertical ^{137}Cs distribution showed a distinct maximum between 8 and 9 cm (Fig. 3A); we interpreted this interval to be 1964, the year of technogenic radionuclide deposition after ground-based nuclear tests in 1961 (Walker, 2006). The ^{210}Pb profile is well approximated by an exponential function (Fig. 3), indicating constant sedimentation conditions and no redeposition of sedimentary material.

The uniform structure of the sediments along the entire core indicated their relatively constant accumulation rate. The approximation of radiocarbon dates to the sediment surface gave a value close to zero (Fig. 3, Table 1), so the reservoir effect for this lake was considered negligible and taken as zero.

Elemental composition

The XRF-SR scanning of the core produced uniform profiles of the vertical Cr, Ga, Ni, V, Pb, U, and Th distributions, which meant they were not informative for our study. PCA distinguished two main groups of elements (Fig. 4): Group I included K, Ca, Ti, Rb, Sr, Zr, Y, and Nb and is related to the PCA 1 axis (46.8%); Group II included Mo, Br, Zn, Cu, and As (Fig. 4). Fe gravitated towards Group I, whereas Mn showed the greatest difference in behavior from all the other elements (Fig. 4).

Selected profiles shown in Figure 5 provide information on shifts in the allochthonous input (Ti), organics (Br), and oxic/anoxic conditions (Fe, Mo, Mn).

Br and Fe data were normalized to Ti because they could be incorporated into the lake from the surroundings, whereas Ti remained stable once deposited in the lake bottom and served as an unambiguous indicator of allochthonous inputs (Vegas-Vilarrúbia et al., 2018). In our case, Ti was used as a common reference, while Fe/Ti, Mn/Fe, and Mo/Mn were used as well-known indicators of redox conditions.

Ti is strongly correlated with Rb, Sr, Y, Zr, Cr, Y, and Nb, which are also known as indicators of surrounding-rock weathering, associated mainly with chemogenic and terrigenous-clastic processes and indicative of allochthonous clastic input (Vegas-Vilarrúbia et al., 2018; Sorrel et al., 2021). Fe was also used as an indicator of allochthonous input (Sorrel et al., 2021). Moreover, Mo may have been associated with organics as well.

Based on the distributions of all the elements, the sediment core was divided into seven zones based on the cluster analysis confirmed by PCA (Fig. 5).

In zone G I (1900–1600 BP), corresponding to the denser sediments, the Fe/Ti and Mn/Fe ratios were the highest in the core, whereas that of Mo/Mn was the lowest (Fig. 5). Other elements had no variations in G I, so this zone corresponded to oxidation conditions, a probable low water level, and a relatively low primary production.

In zone G II (1600–1200 BP), the Fe/Ti and Mn/Fe ratios significantly decreased, while that of Mo/Mn increased, indicating more reduced conditions. The sediments became less compact.

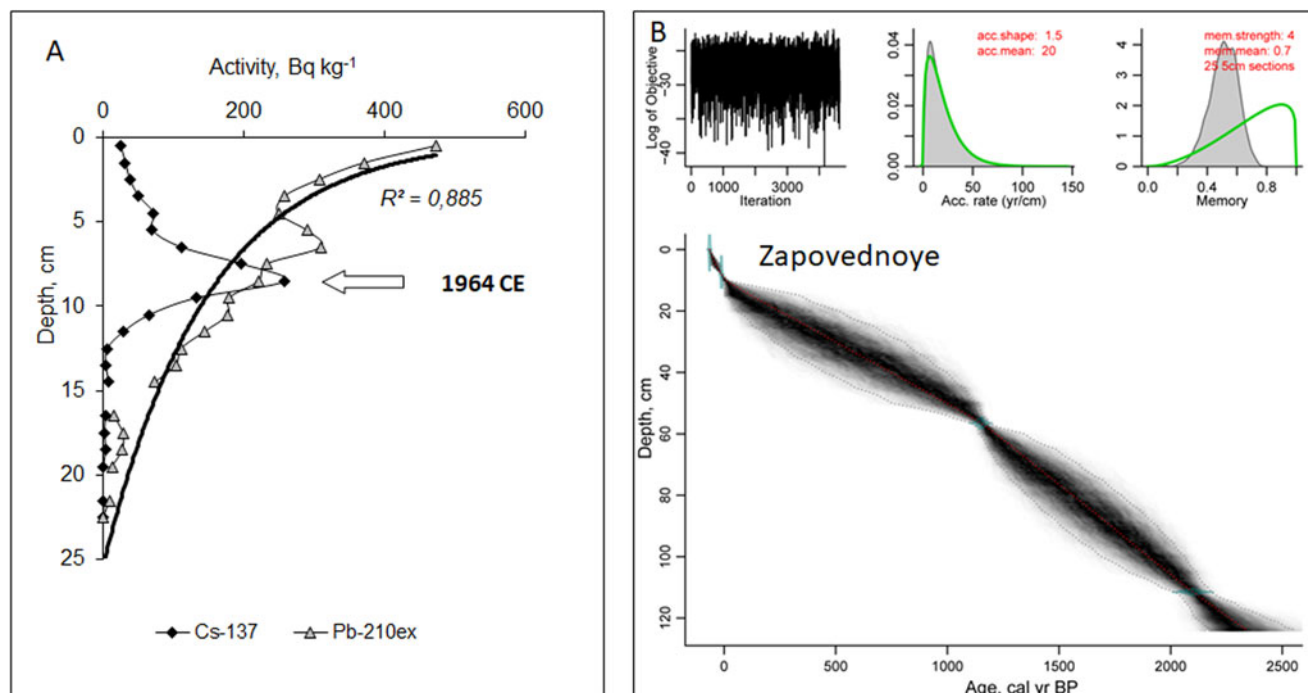


Figure 3. (A) Vertical distributions of ^{137}Cs and ^{210}Pb activity in the bottom sediments of Lake Zapovednoye. (B) Age model and calibrated radiocarbon dates for the bottom sediments of Lake Zapovednoye.

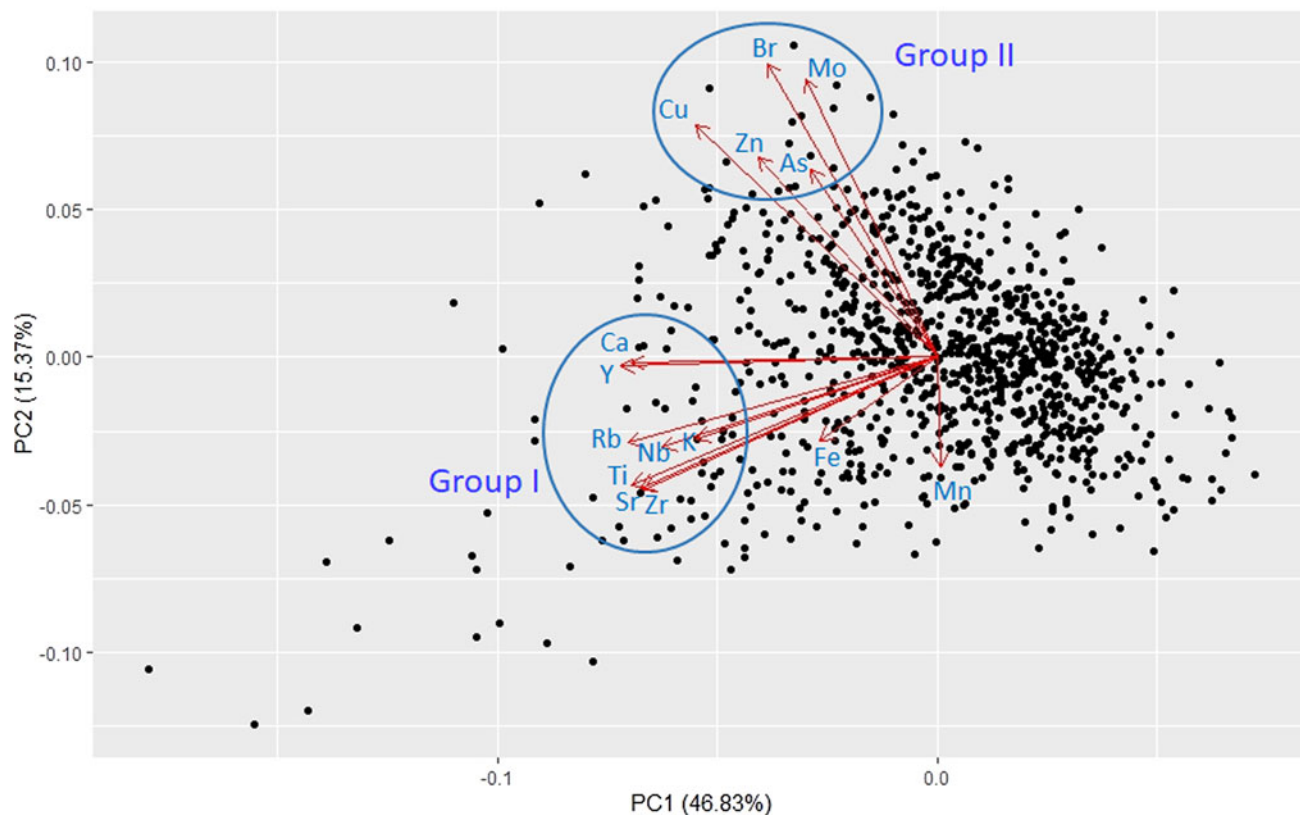


Figure 4. PCA biplot illustrating the distributions of chemical elements in the sediment core of Lake Zapovednoye. The black dots indicate samples, arrows chemical elements.

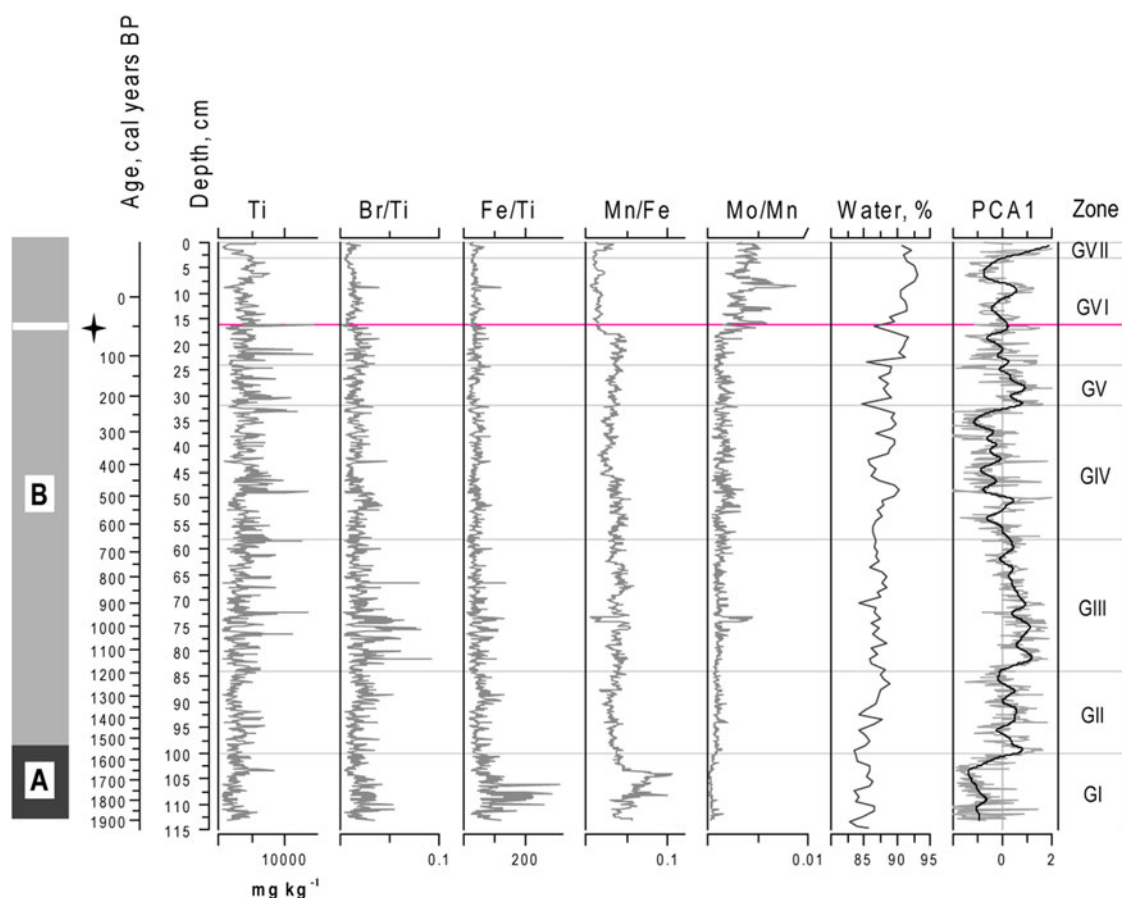


Figure 5. Vertical distributions of Ti and selected element ratios obtained from the X-ray fluorescence (XRF) measurements of the bottom sediments of Lake Zapovednoye. The gray lines present XRF-SR scan data; the black ones are fitted by LOESS smoothing with span 0.5. The horizontal pink line shows the sediment layer of the 1908 Tunguska impact event.

In zone G III (1200–600 BP), Br/Ti increased along with fluctuations in Ti and Br/Ti, while the ratios of Mo/Mn, Fe/Ti, and Mn/Fe remained unchanged. The amplitude and frequency of variations in K, Ca, Ti, Rb, Sr, Zr, Y, and Fe increased.

In zone G IV (600–200 BP), all the profiles remained almost constant, and a small trend towards a Mn/Fe decrease and Mo/Mn increase was observed. The amplitude of Br/Ti decreased.

In zone G V (200–100 BP), a trend towards a Mn/Fe increase was identified; all other profiles remained constant.

In zone G VI (100 to –50 BP), the Mn/Fe concentrations continued increasing and that of Mo/Mn began to increase. The abrupt changes registered at a depth of 16 cm corresponded to about 1909 CE. There was a visually discernible light gray inter-layer about 3 mm thick, also marked in Figure 5 by a pink band. In this layer, K, Ti, Rb, Sr, Zr, Y, and Nb demonstrate synchronous peaks (Fig. 6). We interpret this layer as corresponding to the Tunguska event (Fig. 6). Above this layer, Mo/Mn increased, while Mn/Fe reduced abruptly along with Br/Ti.

In zone G VII (–50 BP until present), Br/Ti, Fe/Ti, and Mn/Fe increased while Ti decreased.

Pollen

The pollen diagram of the bottom sediments of Lake Zapovednoye was divided into three pollen zones (Fig. 7).

PZ I (2200–1600 BP) was dominated by *Pinus* subgenus *Haploxylon* and *Betula* pollen. The abundance of *Abies* pollen

was also the highest compared to the other zones. However, the percentage of Cyperaceae pollen was lower than in the other zones.

In PZ II (1600–350 BP), *Pinus* and *Betula* pollen dominated while the amounts of *Abies* pollen decreased. The percentage of herbaceous plants increased slightly, e.g., *Artemisia* and Poaceae. Notable was the appearance of *Larix* pollen.

PZ III (350 to –64 BP) was characterized by an increased abundance of *Pinus* and *Betula*; the proportion of herbaceous plant pollen was similar to that in PZ II. The percentage of *Picea* pollen in this zone decreased. *Abies* pollen disappeared in the middle of the zone, but then its amount increased considerably.

At a depth of 16 cm (ca. 1908 CE), pollen concentration increased.

Chironomids

In total, 84 chironomid taxa were identified. Chironomid communities of the investigated core were very diverse, with N2 varying from 24.4 at the bottom of the core (ca. 2200 to 1900 BP) to 13.0 at ca. 1983 CE. The median N2 is 18.2. The chironomid record was subdivided into four chironomid assemblage zones (Fig. 8).

In CH I (2200–1600 BP), the chironomid communities consisted of taxa characteristic of moderate temperature conditions (*Tanytarsus pallidicornis*-type, *Microtendipes pedellus*-type) and cold-stenotherm taxa (*Tanytarsus chinensis*-, *Micropsectra*

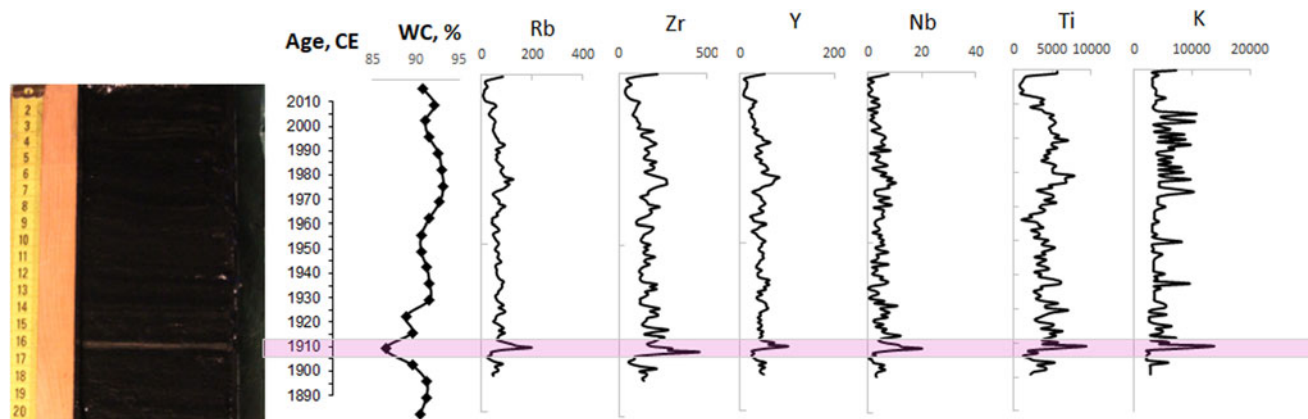


Figure 6. Photo, water content (WC, %) and XRF core-scan (ppm) of the upper section of core ZAP-1. The light gray layer corresponds to the date of the 1908 Tunguska impact event.

insignilobus-, and *Corynoneura arctica*-types). The taxa characteristic of flowing water (*Tvetenia bavarica*-, *Eukiefferiella fittkaui*-, and *Nanocladius rectinervis*-types and *Synorthocladius*), indicative of water-level fluctuations, as well as the semiterrestrial taxa *Limnophyes*–*Paralimnophyes* were well represented. Many taxa from the genera *Limnophyes* and *Paralimnophyes* live in rapidly changing environments and are often found in semiterrestrial conditions. These detritivorous taxa live mainly near the water surface and among thickets of vegetation (Brooks et al., 2007; Moller Pillot, 2013).

In CH II (1600–800 BP) after 1400 BP, the abundance of *M. pedellus*-type increased to 12.5% and remained high throughout this zone. As a rule, this taxon is widely distributed in stagnant or slow-flowing water bodies with a high oxygen content and low nutrient load in temperate climatic conditions. Some species

from this group are acid tolerant (Moller Pillot, 2013). Many taxa that prefer to live among macrophytes, including in flooded areas, were present in this zone and include *Polypedilum nubeculosum*-, *Cricotopus intersectus*-, *Cladotanytarsus mancusi*-, *E. fittkaui*-, and *Co. arctica*-types, *Paratanytarsus*, etc. After 1000 BP, there was a decline in *M. pedellus*-type and an increase in the taxa characteristic of colder climates and oligotrophic conditions. These included *Mi. insignilobus*-, *Paratanytarsus penicillatus*-, *T. chinyensis*-, and *Nanocladius branchiculus*-types. The number of species characteristic of flowing water decreased, except for *Tv. bavarica*-type, which was numerous at about 1500 BP and fell thereafter.

In CH III (800–300 BP), the abundance of *Limnophyes*–*Paralimnophyes* and *Co. arctica*- and *Cricotopus cylindraceus*-types increased compared to the previous period.

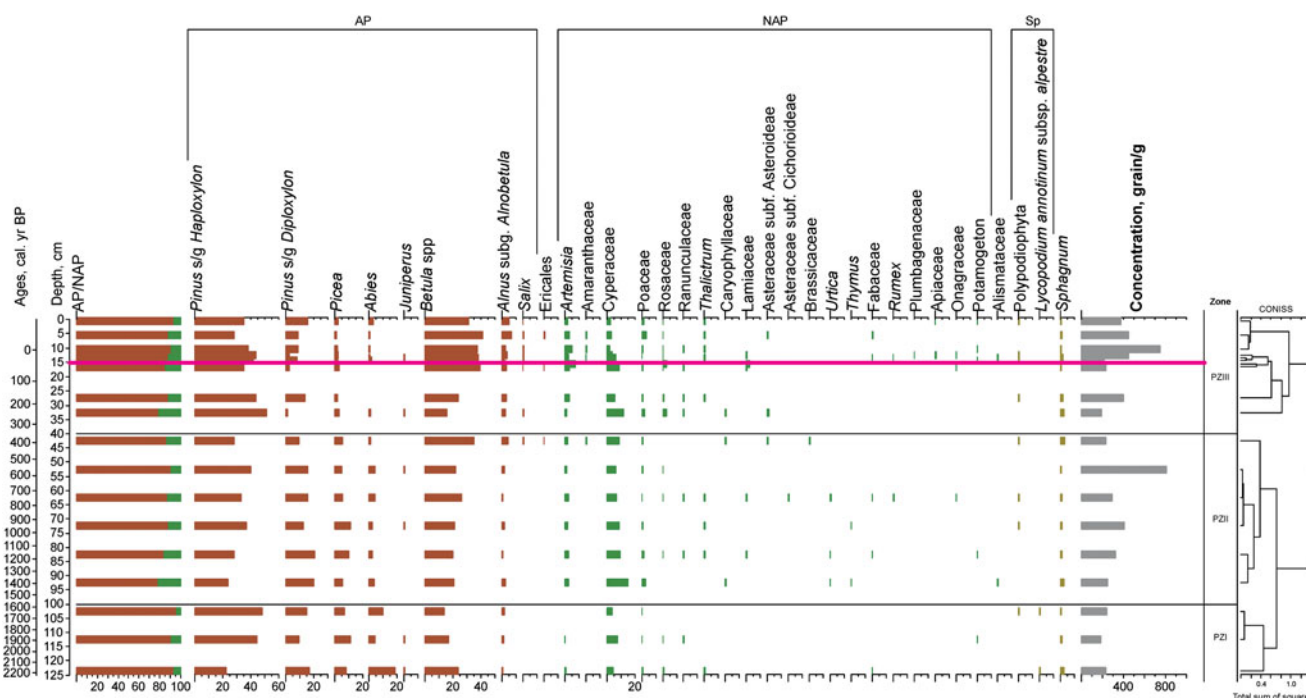


Figure 7. Pollen diagram for Lake Zapovednoye. Horizontal red line shows the sediment layer of the 1908 Tunguska impact event. AP, arboreal pollen; NAP, non-arboreal pollen; Sp, spores.

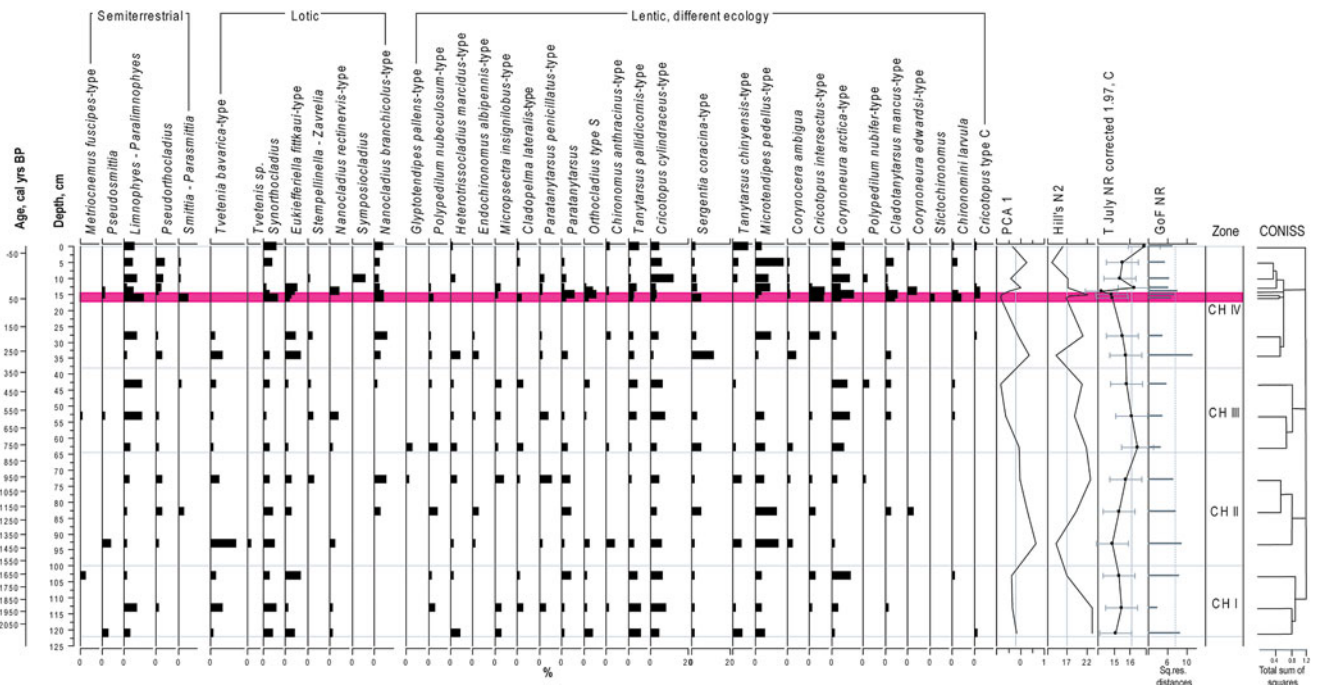


Figure 8. Relative proportions of the most abundant chironomid taxa in the sediments of Lake Zapovednoye, PCA axes 1 scores for chironomid data, N2 diversity, chironomid-inferred T July, and goodness-of-fit results (squared residual distance) tests for reconstructed T July, with 95th percentile of the residual distances of all the modern samples that are identified as samples with a “poor fit” with the reconstructed T July (dashed line). Horizontal red line shows the sediment layer of the 1908 Tunguska impact event.

However, the abundance of some other species indicative of flowing water decreased (*Synorthocladius*, *Tv. bavarica*-type, *Nanocladius* taxa, *Eukiefferiella*).

In CH IV (300 to –64 BP), two intervals could be distinguished in this zone: from 300 to ca. 50 BP, and from ca. 50 BP to –64 BP. At the beginning of the first interval, at about 250 BP, there was a sharp increase in such cold-condition taxa such as *Sergentia coracina*-type and *Corynocera ambigua* that prefer mainly cold oligotrophic lakes, which may have indicated climate cooling as well. This interval probably corresponds to the Little Ice Age.

Around the depth of 16 cm that, according to our age model, corresponded to 1904 ± 5 CE, we observed a substantial shift in the taxonomic composition and strong short-term rise in the diversity of chironomids, which was also indicated by a sharp decrease in the values of the PCA 1 axis. At this time, the number of taxa indicative of flowing water (*Synorthocladius*, *Nanocladius*, *Eukiefferiella*) and of unstable water level or shoreline erosion (terrestrial and semiterrestrial taxa; *Limnophyes*–*Paralimnophyes* and *Smittia*–*Parasmittia*) increased significantly. After about 40 BP, the number of oligotrophic *M. pedellus*-type and other taxa, also characteristic of moderate temperatures (*Eukiefferiella claripennis*-, *T. pallidicornis*-, and *Cr. intersectus*-types) rose.

Cladocera

A total of 30 cladoceran taxa were found in the subfossil Cladocera community of Lake Zapovednoye, of which 23 were identified to the species level. Such species as *Camptocercus fennicus*, *Camptocercus lilljeborgi*, and *Phreatolona protzi* were new for the region. Throughout the studied period of the history of the lake, the community was dominated by planktonic species.

Benthic or lithophilic taxa were much less represented, reflecting the predominance of pelagic biocenoses over the littoral zones and a considerable lake depth. Also, in the CZ I–CZ III cladoceran zones, the species *P. protzi* indicative of flowing water was found. The community was dominated by the taxa preferring neutral pH conditions and indicative of oligo- and mesotrophic conditions. Four Cladocera zones were distinguished (Fig. 9).

CZ I (2200–1100 BP) is characterized by a clear dominance of the planktonic taxa *Bosmina longispina* (59–78%) preferring cold and temperate conditions. The taxon is very sensitive to changes in the trophic status of the environment and can serve as an indicator of oligotrophic and oligosaprobic conditions (Flöbner, 2000). In the lower part of the core, a high proportion of the relatively warm-water taxa *Leptodora kindtii* and *Camptocercus rectirostris* (up to 7%) was detected, the abundances of which decreased towards the top part of the zone (Fig. 9).

Around 1350–1200 BP, a rare oligosaprobic cold-stenotherm taxon *Ophryoxus gracilis* was found. The species has a northern distribution and is most common in the littoral zone of lakes; it is indicative of oligotrophic conditions and relatively electrolyte-poor waters (calcium $[Ca^{2+}]$ concentrations <26 mg/L) (Flöbner, 2000). The presence of the rare and highly specialized taxon *P. protzi*, typical of flowing or interstitial waters, indicated that the lake was influenced by flowing water (Frolova et al., 2019).

CZ II (1100–500 BP) is characterized by changes in the dominant taxon: *Daphnia longispina* gr./*Ceriodaphnia* sp. increased up to 60% and became dominant while the true planktonic taxa of *B. longispina*-type decreased down to 20%. The abundance of littoral, cold-stenothermic, or the so-called “northern” taxa (Harmsworth, 1968) *Acroperus harpae* and *Biapertura affinis* attained maximal occurrences in the core (approx. 7% and 2%, respectively) at the top of CZ II after 600 yr BP.

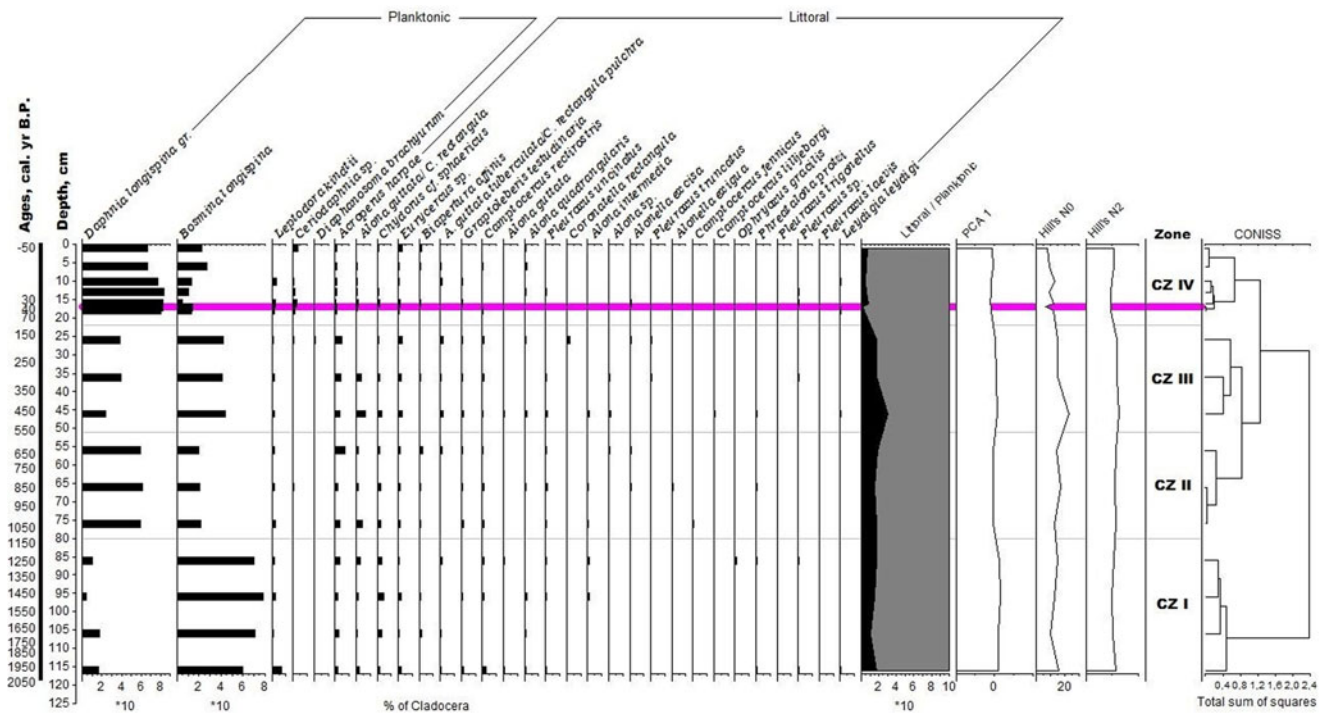


Figure 9. Cladocera taxa in the sediments of Lake Zapovednoye, ratio of littoral and pelagic species, PCA axes 1 scores for cladoceran data, and N2 diversity. Horizontal purple line shows the sediment layer of the 1908 Tunguska impact event.

In CZ III (500–100 BP), the cool-water planktonic taxa *B. longispina* increased to 40%, while the proportion of more warm-water *Da. longispina* gr./*Ceriodaphnia* sp. decreased to 20–40%. In the beginning of the zone, the number and abundance of littoral taxa including cold-water *A. harpae*, *Alona guttata*, and *Coronatella rectangula* increased. These changes in the composition of cladoceran communities after 600 BP at the end of CZ II and CZ III probably indicate a deterioration in the climatic conditions and reflect the harsher conditions of the Little Ice Age.

In CZ IV (100 to –64 BP), substantial changes led to yet another change of the dominant taxa in the cladoceran community when the oligosaprobic and cold-water *B. longispina* was replaced again by *Da. longispina* gr., preferring more moderate conditions. *Daphnia longispina* gr. composed from 66.0 to 82.2% of the total abundance of cladoceran remains in this zone. Around the depth of 16.5 cm, during the period corresponding to the Tunguska event, we observed a prominent shift in the composition of cladoceran communities, namely a decrease in the PCA 1 values, reflecting a sharp decrease in species richness. The cladoceran taxa in this layer drop to six, although generally, for CZ IV, the number varied from 8 to 13. The changes occurred primarily due to the loss of the littoral taxa (Fig. 9), mostly closely associated with littoral vegetation (*Eurycercus* sp., *Bi. affinis*, *Ca. rectirostris*) that reappeared in the lake in subsequent layers. Water flow indicators were not found in this zone, which may be only due to the relative rarity of such indicators among cladocerans.

In the uppermost sample there was an increase in the abundance of littoral taxa, such as *Eurycercus* sp. and *Ceriodaphnia* sp., closely associated with well-developed littoral vegetation.

Diatoms

Cluster analysis divided the Zapovednoye Lake core into four diatom zones (Fig. 10).

Zone D I (2200–1100 BP) contains a complex of planktonic–benthic species dominated by *Tabellaria fenestrata*. Although this zone was characterized by the lowest proportion of benthic species in the core, the benthic *Staurosirella pinnata* was among the dominant ones. Within D I, we observed a clear increase in the proportion of planktonic species (*Ta. fenestrata*, *Aulacoseira granulata* var. *angustissima*) to reach the highest abundance in the core.

Lindavia lemanensis was subdominant in the lower part of the zone, but increased significantly and became dominant in the upper part of the zone. The proportion of the small pennate diatoms *S. pinnata*, *Staurosira venter*, and *Pseudostaurosira elliptica* decreased in this zone.

The lower part of the zone is dominated by halophobous and salinity-indifferent species preferring alkaline conditions, while the proportion of acidophilic species increased towards the top of the zone. The dominant species were cosmopolitan, but the arctic–alpine species *Aulacoseira valida* and cold-stenotherm *Diploneis parva* were present in small numbers.

The diatom composition of D I is indicative of flowing water with low mineralization under cool temperature conditions. There was also a tendency towards increasing water levels and the formation of a zone of acidic shallow waters.

Zone D II (1100–350 BP) is characterized by an increase in the proportion of halophilic and alkaline species while the abundance of the halophobous planktonic–benthic *Ta. fenestrata* decreased, to be replaced by another halophobous planktonic–benthic species, *Meridion constrictum* Ralfs, that prefers alkaline environments. Abundances of the alkaliphilic species *Aulacoseira ambigua*, *Au. granulata* var. *angustissima*, and *Aulacoseira subarctica* gradually increased alongside the increasing proportion of benthic species dominated by *S. pinnata*, *Unaria ulna*, and the planktonic–epiphytic *Fragilaria vaucheriae*. In the upper part of the zone, the highest increase in the proportion of *Discostella stelligera* for

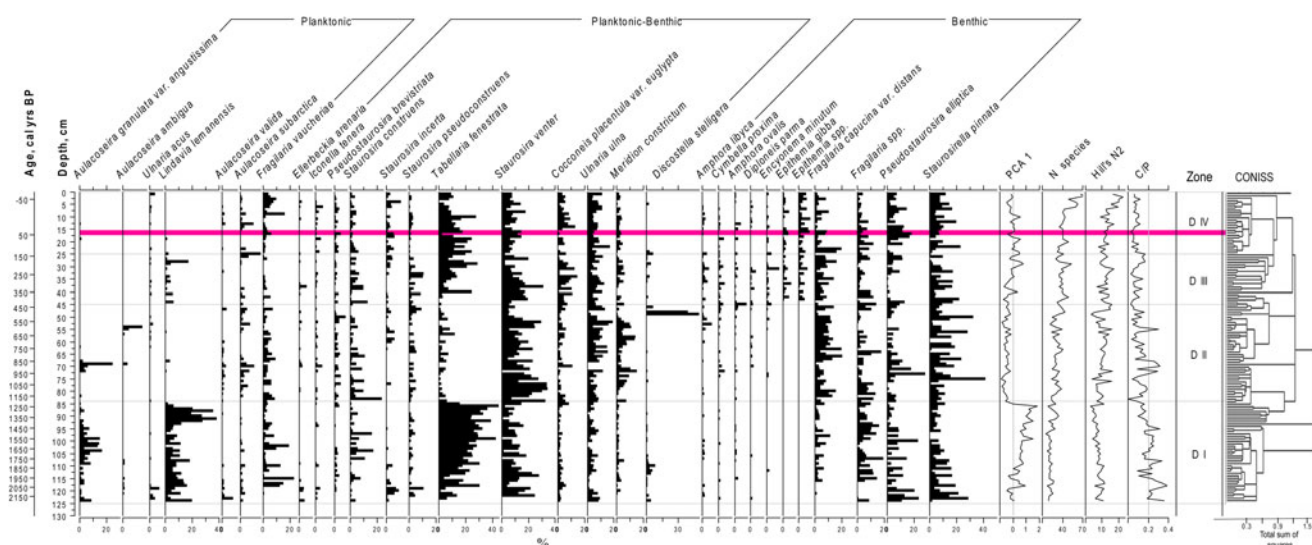


Figure 10. Most abundant diatom taxa in the sediments of Lake Zapovednoye, PCA axes 1 scores for diatom data, N2 diversity and N for the number of taxa. C/P is Centric/Pennate diatoms ratio. The horizontal red line shows the sediment layer of the 1908 Tunguska impact event.

the entire core was detected. The findings indicate the lake had a high and constant level of warm water of increased productivity.

Zone D III (350–100 BP). Within this time interval, the trend was towards an increase in the abundance of planktonic–benthic species dominated by *Ta. fenestrata* and *Cocconeis placentula* var. *euglypta* and benthic species dominated by *S. pinnata*, *St. venter*, and *U. ulna*. The planktonic species *L. lemmanensis* and *Au. subarctica* were found to dominate in this zone. However, at the top part of the zone, the proportion of *C. placentula* var. *euglypta* reduced to be replaced by *L. lemmanensis*. Moreover, such taxa as *Encyonema minutum*, *Epithemia gibba*, and *Epithemia* spp. appeared for the first time. The zone was characterized by an increase in the proportion of halophilic species and the preservation of weakly alkaline conditions. The cold-stenotherm *Di. parma* was constantly recorded within the zone. The diatom composition reflects a cooling environment, stable or lowered water level, and increased mineralization.

Zone D IV (100 to –67 BP). The proportion of benthic and planktonic–benthic species, predominantly halophilic and alkali-philic, continued to increase with such species as *Ta. fenestrata*, *S. pinnata*, *St. venter*, and *U. ulna* becoming dominant, which may have reflected the lowering of the water level, a warmer environment, more alkaline water, and shallow-water littorals overgrown by macrophytes. Mineralization remained similar to that in D III.

There was only a slight taxonomic shift in the diatom assemblages corresponding to ca. 18 cm, or ca. 1908 CE, reflected as well by PCA 1 (Fig. 10). The abundance of *Ta. fenestrata* dropped from 24 to 2%, *S. pinnata* from 10 to 0–4%, and *U. ulna* from 9 to 4%. At the same time, the abundances of otherwise less-abundant species grew for a short time: *F. vaucheriae* (2 to 6%), *Fragilaria capucina* var. *distans* (2 to 9%), *Ps. elliptica* (8 to 18%), *Stauroneis incerta* (0 to 6%), and *St. venter* (6 to 15%). However, the diversity of diatom assemblages remained similar to those found in adjacent sediment layers.

Mean July air temperature reconstruction

The application of the chironomid-based NR transfer function resulted in reconstructed T July fluctuations of approximately

2.4°C over the last ca. 2.2 ka (Fig. 8) with the lowest temperatures (14–15°C) reconstructed for the period between ca. 200 BCE and 650 CE, and gradual warming towards 950 CE with the warmest T July calculated between ca. 1000 and 1350 CE (max T July 16.5°C, median T July 15.6°C). There were coolings between ca. 1690 and 1920 CE (median T July 14.1°C), and T July rose to 16.8°C in the more recent period, which is close to the modern T July, taking into account the RMSEP of the applied model (1.43°C).

All 77 identified chironomid taxa were represented in the modern training sets. Three of 77 taxa had a Hill's N2 < 5 and therefore were defined as not well represented in the training sets: *Tv. bavarica*-type (N2 = 2 in the NR data set and 8.8 in the core), *Synorthocladius* (N2 = 1 in the NR data set and 12.4 in the core), and *E. fittkaui*-type (N2 = 1 in the NR data set and 12.1 in the core). These three taxa were frequently found in the core, and their low representation in the NR data set hampered the reconstruction quality, which is confirmed by GoF statistic results. GoF for T July reconstruction revealed that five samples had a “poor” fit with the temperature (Fig. 8), while the rest of the samples showed either a “good” or “moderate” fit. The poorest fit was demonstrated by the sample at ca. 1700 CE containing *Tv. bavarica*- and *E. fittkaui*-types, the taxa of high abundance that were poorly represented in the NR data set. The high representation of the taxa in the training set and primarily good GoF results indicated that the temperature reconstruction from the Lake Zapovednoye record was reliable. However, the samples with poor GoF tests should be interpreted with caution.

DISCUSSION

Lake morphology

The rounded-funnel-shape of the lake, its significant depth, and large depth/diameter ratio indicate its origin is not associated with thermokarst processes (Rogozin et al., 2023). Two other lakes of unknown origin and similar shape, Cheko (Gasperini et al., 2007; Rogozin et al., 2017) and Peyungda (Rogozin et al., 2023), have been described in the vicinity of Zapovednoye. According to one version, Lake Cheko is a crater from the fall

of a cometary body at the time of the Tunguska event (Gasperini et al., 2007), but others assert that the lake is older than the 1908 Tunguska impact event (Rogozin et al., 2017). The similar funnel shape, large depth-to-diameter ratio, and location of river channels indicate all three lakes have a similar origin that is geologic rather than impact in nature. However, the question about the origin of these lakes remains open. Seismoacoustic studies have shown that the bottom sediment thickness of Lake Zapovednoye is about 4 m, and that of Lake Peyungda is over 6 m, meaning the age of both lakes spans several thousand years (Rogozin et al., 2023).

Seismoacoustic profiling of the littoral slopes of Lake Zapovednoye has revealed several horizontal “shelves” covered in sediments (Rogozin et al., 2023), which means its basin could have subsided gradually increasing the lake volume and depth. Therefore, the bottom sediment composition could be affected directly by climatic factors but also indirectly by basin subsidence that may have occurred as a result of geologic factors.

Reconstruction of the climate and limnological conditions

The biological and geochemical data obtained during our study make it possible to discuss several environmental and ecological aspects of Lake Zapovednoye such as temperature, lake level fluctuations, water flow, terrigenous material input, redox conditions, and trophic status. Figure 11 summarizes the results for all the proxies and shows several event boundaries.

The time intervals of statistically significant zones for the different proxies do not coincide in the studied core, but the most prominent periods have been confirmed by several paleo-indicators. The climatic changes are most clearly seen in the chironomid-based T July profile (Figs. 8 and 11). The identified temperature changes are consistent with those from neighboring Siberian regions and reflect the known trend of alternating cold and warm periods in northern Eurasia (Fig. 11).

During approximately the last 1600 years, neither the climate nor the environment have changed much, which is generally

consistent with published paleoenvironmental reconstructions for Central Siberia that cover a similar period (i.e., Glückler et al., 2022). However, the lowest layers of the core, separated by a clear boundary at a depth of about 94 cm (ca. 1600 BP), differ markedly from its other parts. Below we provide a chronological description of the major changes in the external conditions of the lake and its ecosystem identified from a combination of examined proxies.

Lower zone: 2200–1600 BP

As inferred from the chironomids, T July before 1600 BP was lower than it is today. The composition of cladoceran communities during this time interval confirms cool climatic conditions. The presence of lotic species of chironomids and Cladocera can indicate that the influent river had stronger runoff. The absence of a developed littoral zone and a small amount of littoral vegetation is strengthened by the apparent dominance of planktonic species among the Cladocera. The rare oligosaprobic cold-stenotherm taxon *O. gracilis*, indicative of electrolyte-poor water (Smirnov, 1971; Flößner, 2000), and another rare and highly specialized taxon *P. protzi* that inhabits flowing or interstitial waters (Frolova et al., 2019), support the presence of rivers flowing into and out of the lake.

The dominance of the oligotrophic diatom species *Ta. fenestrata* may also indicate water flow (Trifonova, 1990). The appearance and dominance of the benthic species *S. pinnata* reflects water mixing, water-level fluctuations, and the influx of nutrients from the catchment (Watchorn et al., 2008). The decreased proportion of this species reflects the stabilization of environmental conditions, decreasing water inflow, and mixing.

However, it could have been that the greater flow was due to a smaller lake volume and not to intensive rainfall. At the same time, the signs of water-level fluctuations in the chironomid and diatom compositions testify in favor of more intense precipitation. The abundance of the hydrophilic *Abies* may also be indicative of a more humid climate in that period. However, it

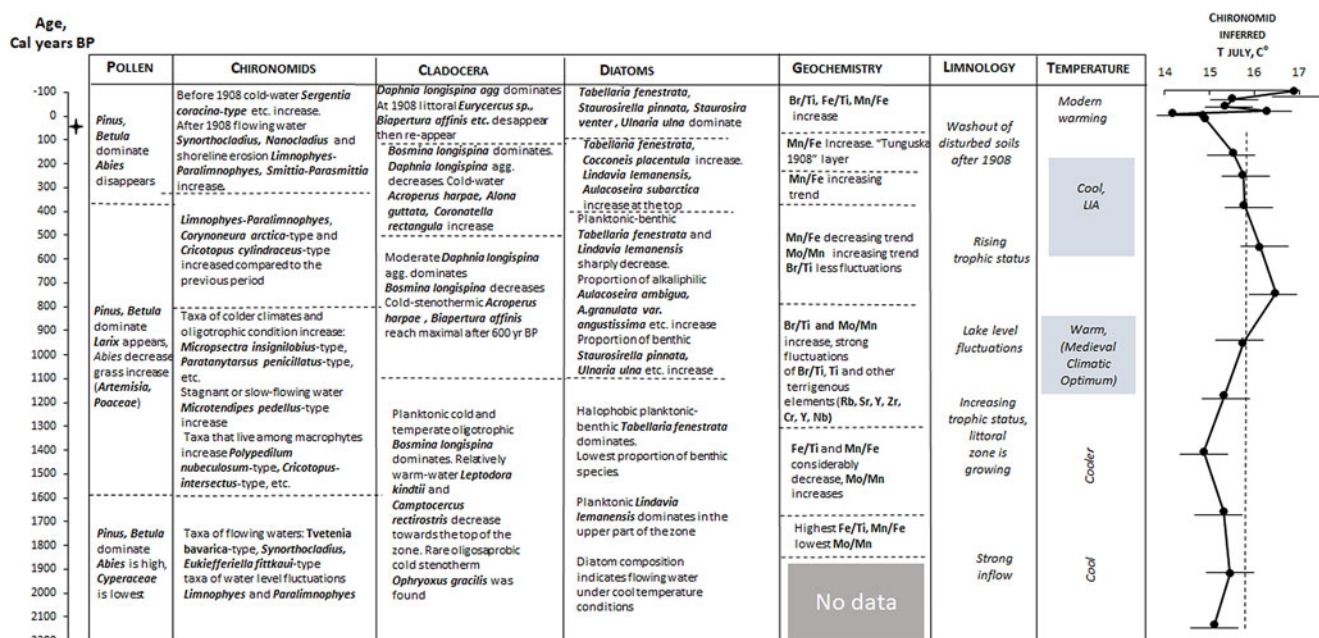


Figure 11. Summary of environmental and ecosystem changes reconstructed from the sediment proxy of Lake Zapovednoye. LIA, Little Ice Age.

is unknown which of the factors, temperature or humidity, controlled its dynamics to a greater extent. Since *Abies* does not grow on dry or waterlogged soils (Burlakov et al., 2009), its disappearance during the latter periods could be a consequence of cooling and/or drying up or waterlogging of the soil. Given that only three pollen samples have been detected in the lowermost pollen zone (2200–1600 BP), one should be cautious about making conclusions based on these scarce data.

Before 1600 BP, the high iron and manganese content (presented as Fe/Ti and Mn/Fe) was a clear sign of an oxidative environment, indicating an ecosystem with intensive water flow (Wirth et al., 2013; Vegas-Vilarrúbia et al., 2018). Fe and Mn are generally assumed to behave similarly in lake water environments, except when Mn precipitates at a higher redox potential than that of iron (Klemm et al., 2015). Fe and Mn become increasingly soluble in reducing lake conditions, with Mn more readily reduced than Fe under anaerobic conditions (Klemm et al., 2015; Vegas-Vilarrúbia et al., 2018). Hence, an increase in Mn/Fe is related to lake water mixing, and may serve as an indication of, e.g., water depth or wind-speed variations. The Mn/Fe ratio is assumed to reflect the lake water mixing of, i.e., the supply of oxygen to the water–sediment interface. Based on these same properties, increases in Fe/Ti ratios have been interpreted as enhanced oxic conditions. Reduced mixing may have occurred during times of more stable lake conditions with relatively higher water levels. Br is considered a tracer of organic content in sediments (Klemm et al., 2015; Vegas-Vilarrúbia et al., 2018; Baisheva et al., 2024).

Mo is readily scavenged under sulfidic conditions, and therefore is a well-established proxy for reduced conditions and the presence of sulfide in the water column (Wirth et al., 2013), whereas enhanced Mn content signifies oxic conditions (Vegas-Vilarrúbia et al., 2018). For that reason, the Mo/Mn ratio best reflects changes in the redox potential of the lake. A low Mo content is also a sign of oxic conditions (Wirth et al., 2013; Zhen et al., 2020). It is possible that between 2200 and 1600 BP, the lake basin had not yet taken its modern form. The lake could have been shallower and smaller in size, which probably ensured a greater water flow, a more oxic environment in the near-bottom water layers, a small area of the littoral zone, and a lower density of littoral vegetation that is confirmed by the composition of the chironomid fauna including more taxa preferring lotic conditions (Fig. 11). Some discrepancy between the pollen and chironomid reconstructions could have resulted from the fact that chironomids respond most to the mean July air temperatures (Nazarova et al., 2023), while vegetation reacts not only to temperature fluctuations but, in inland Siberia, also to changes in complex climate–permafrost–fire–vegetation interactions (Cao et al., 2019). Consequently, the decrease in average annual temperature detected by pollen may be accompanied by an increase in the July temperatures detected by chironomids, if climate continentality had increased. In general, the results of our multiproxy analysis suggest that this period can be characterized as relatively cool and humid.

Middle zone: 1600–350 BP

An evident change in the ecological conditions can be traced for a period after 1600 BP. During this time, the amount of precipitation might have fluctuated significantly, which led to an uneven supply of allochthonous matter and surface runoff. As a rule, a slight increase in Br is associated with increased organic matter (Fedotov et al., 2013) and may also indicate an increase in lake

productivity. On the other hand, a decrease in Fe and Mn is indicative of a reduced flow and a possible increase in the trophic status of the lake. An increase in the frequency and amplitude of fluctuations in Ti, Rb, Sr, Zr, and Y concentrations indicates unstable conditions. These elements are usually associated with clastic indicators of weathering in surrounding rocks (Vegas-Vilarrúbia et al., 2018; Sorrel et al., 2021).

An increase in Mo/Mn, indicative of reducing conditions often associated with organic matter (Wirth et al., 2013), was observed after ca. 1100 BP. Most likely, it also indicates a further decrease in the oxygen content of the water column, which may have been a consequence of warming and/or an increased trophic status of the lake (Wirth et al., 2013). It may also have been due to the development of an anaerobic hypolimnion related to the lake's increased depth. The decrease in *Abies* pollen and *Larix* appearance are indicative of a cool climate and low humidity.

Between 1000 and 350 BP, a shift towards more mesotrophic chironomid taxa was observed, and the chironomid-inferred temperature reached a maximum of ca. 1.5°C above the modern level. The thermophilic species that appeared in the zooplankton were also indicative of warming. At the same time, the decrease in the planktonic taxa of the cladoceran community suggests a change in the ratio of deep pelagic and littoral shallow areas in favor of the latter. If compared to the earlier sediment layers, the species richness of cladoceran remains in the bottom sediments increased, indicating the community had become more complex and balanced under the relatively favorable conditions in the presence of diverse biotopes.

Analysis of the diatoms also showed signs of warmer conditions, as indicated by *Au. ambigua*, *Au. granulata*, and their varieties (Trifonova, 1990; Stenina, 2009). There was also a succession of diatom species from a poor planktonic assemblage dominated by the planktonic, centric, acidophilic, and halophobic species of diatoms preferring high mineralization, biogenic elements, and pH. The high abundance of *D. stelligera* indicates an increase in trophic status (Trifonova, 1990) and/or pH (Camburn and Charles, 2000). A significant increase in *D. stelligera* could also have been associated with a decrease in the water level in the lake and an increase in mineralization following the warming. This period presumably corresponds to the Medieval Climate Optimum.

Top zone: 350 BP–current time

The observed decrease in Mo, indicative of a more oxic environment, may have reflected the cooling of the lake associated with a decrease in its trophic status. The cold-water chironomid and cladoceran taxa that appeared at ca. 350 BP and a total disappearance of *Abies* between 300 and 100 BP could have been related to the cooling corresponding to the Little Ice Age. Among the diatoms, the return of the freshwater epiphyte *Ta. fenestrata* to its dominant position reflected the lowering of the water level and the formation of shallow-water zones overgrown by macrophytes (Patrick and Reimer, 1966).

In the more modern time, after 100–50 BP, an increase in *Betula*, *Pinus*, and herbaceous pollen proportions, an almost complete disappearance of *Larix* pollen, and a decrease in *Picea* may indicate climate warming in the region.

Thermophilic cladoceran species, such as *Le. kindtii*, also appeared. In the chironomid communities, a shift occurred from cold-stenotherm to more temperate species. The decline in *Se. coracina*-type and an increase in the chironomids indicative of moderate conditions after 0 BP indicate climate amelioration.

Thus, the composition of sediments and shifts in biological communities during the twentieth century reflects the transition from the Little Ice Age to modern warming.

Traces of the 1908 Tunguska impact event

The investigated core had a geochemical anomaly observed at the depth corresponding to ca. 1908 CE. The layer was visually distinctive and enriched with the elements indicative of terrigenous inflow (Fig. 6). We assume the layer originated due to the 1908 Tunguska event. This powerful atmospheric explosion that happened on June 30, 1908, caused a forest fire of about 700 km² and felled the forest trees around the epicenter in an area of about 2200 km² (Vasiliev et al., 2003; Gladysheva, 2020). According to the chronicles, observations following the event, and further investigations, the density of the fallen trees at the border of the fire zone was about 1400 trees per hectare, i.e., on average, one tree fell in a 3 × 3 m plot, and the holes from uprooted trees could reach 3 m in diameter (Abramov et al., 2003) (Fig. 12), which means that the soil was significantly disturbed over a large area leading to increased terrigenous material supply from the catchment (Darin et al., 2020).

Lake Zapovednoye is located about 20 km from the border of the forest fall zone. However, the upper reaches of the Verkhnyaya Lakura River flowing into Lake Zapovednoye are located precisely at the border of this zone, and the terrigenous material could have easily been transported into the lake by the river. It means the layer high in K, Ti, Rb, Y, Nb, and Zr that formed at a depth of 16 cm (Fig. 6) appeared through the increased supply of terrigenous material from the catchment area after the Tunguska event.

No geochemical anomalies, namely elevated concentrations of Ni and Ir, that could be associated with extraterrestrial matter were identified in the lake sediments. The Ni profile was uniform, and that of Ir was not measured in this study.

There were substantial changes in the taxonomic composition of chironomids and Cladocera around 1908 CE. Right after this

time, the chironomid taxa that prefer flowing conditions and are indicative of an unstable water level or soil/coastline erosion (terrestrial and semiterrestrial taxa) appeared. As for the Cladocera, their numbers dropped by almost two times in the period following the Event, and these changes occurred primarily due to the disappearance of the taxa associated with littoral vegetation. Though their abundance was restored in the overlying sediment layers, no flow indicators were detected in this interval, which may have been due to a relative rarity of such indicators among the Cladocera.

The observed short-term decline in pollen concentration is presumably related to the Event. The increased proportions of the valves of several alkaliphile diatom species could have been due to increased reservoir productivity in the specified time period. On the other hand, it may have also been associated with increased turbidity due to intensive surface runoff following the Event. Based on the time interval between adjacent 1 cm samples, it is possible to estimate the rate of recovery of chironomid, cladoceran, and diatom communities after the Tunguska event as 6–10 years. However, communities did not recover to be similar to those pre-Event, i.e., the Event had a more lasting paleoecological effect.

Comparison to the neighboring regions

The earlier reconstructions based on peatland plant macrofossil analysis and soil sections from the Nizhnyaya Tunguska basin (Kutafyeva, 1974; Koshkarova and Koshkarov, 2005; Koshkarov and Koshkarova, 2018) demonstrated that between ca. 2400 and 1600 BP, the studied area was covered in *Picea*, *Larix*–*Pinus*, and *Larix*–*Betula* forests. Similar conclusions were drawn from pollen spectra (Kol'tsova, 1981; Koshkarova and Koshkarov, 2005). The modern period in this region is characterized by the predominance of *Pinus*–*Larix* forests, while until ca. 500 BCE, there were dark coniferous forests, including *Picea* and *Abies* (Koshkarov and Koshkarova, 2018).



Figure 12. Trees knocked down and burned around the site of the 1908 Tunguska impact event. Copied from the *Around The World* magazine, 1931. The original photo was taken in May 1929.

In the pollen spectra of CH-12 (Khatanga-12), a small lake located 1000 km to the north of Lake Zapovednoye at the tree line border of the Taimyr Peninsula (72°N, 102°E), *Larix* was replaced by tundra vegetation at ca. 2000 BP, which indicates a transition from a warmer to a cooler climate (Klemm et al., 2015). In our study, a decrease in the amount of *Abies* pollen and the appearance of *Larix* pollen at about 1600 BP have been observed (Fig. 7). Thus, it is possible that in the pollen spectra of both lakes, there are signs of *Larix* shifting to the south that is indicative of climate cooling. This phenomenon is generally consistent with the Late Holocene cooling observed southeast of the Tunguska basin and in the region of Lake Baikal (Prokopenko et al., 2007; Fedotov et al., 2012).

However, results of chironomid analysis from the same Taymyr core (CH-12) did not show any significant climatic change at ca. 2000 BP, and the reconstructed T July remained similar to the modern one (Syrykh et al., 2017). At about ca. 2500 BP, pollen spectra have shown some warming that started earlier in central Evenkia (Koshkarova and Koshkarov, 2005). A transition from a cold and dry to a warm and humid climate at 2050 BP was reconstructed for Western Siberia (55°N, 82°E) (Krivonogov et al., 2012).

Inferred from the chironomids of Lake Zapovednoye, T July revealed cool conditions until ca. 1400 BP that developed later into a warming trend (Fig. 8). The reconstruction based on chironomids from the small shallow lakes of the Putorana Plateau (68°N, 92°E) demonstrated a cool temperature and an increase in continentality shortly before 2000 BP (Self et al., 2015).

Therefore, we have found that between 2200 and 1600 BP, the investigated area had a humid and cool climate corresponding to the Late Holocene cooling. This period matches well with the cool period observed in Siberia about 2000 years ago that manifested itself by glacier advances in the Altai Mountains (Solomina, 1999; Rudoy et al., 2000; Agatova et al., 2012). The end of this period corresponds to the Late Antique cooling, or the Late Antique Little Ice Age, observed in Europe and the Altai during this period (Büntgen et al., 2016).

Evidence shows that in the more northern regions of Taimyr and Putorana, the warm period between 1100 and 600 BP (Naurzbaev and Vaganov, 2000; Naurzbaev et al., 2002; Syrykh et al., 2017) was followed by cooling (Andreev et al., 2002; Hantemirov and Shiyatov, 2002; Syrykh et al., 2017).

The Medieval Climate Optimum (between ca. 1000 and 700 BP) characterized by strong climatic fluctuations in the Northern Hemisphere was generally relatively warm (Stine, 1998; Mackay et al., 2012). The warm period preceding 700 BP and followed by a sharp cooling in the Eastern Sayan mountains is evidenced by the taxonomic composition of and the mean T July inferred from chironomids (Mackay et al., 2012). This reconstruction is generally consistent with the T July reconstructed from chironomids and signals from other bio- and geochemical proxies of Lake Zapovednoye. Tree rings (Naurzbaev and Vaganov, 2000; Naurzbaev et al., 2002) and glaciomarine sediment records (Zeeberg et al., 2003) indicate the climate became cooler in Northern Siberia during this period.

The T July inferred from chironomids from the lakes of the Putorana Plateau has also shown climatic warming during the last 50 years (Self et al., 2015). Signs of modern warming have been found in the sediments of many lakes in Northern Siberia (Nazarova et al., 2013; Biskaborn et al., 2015 and references therein). In the southern part of Eastern Siberia, a sharp transition from the Little Ice Age to modern warming was observed (Fedotov et al., 2013).

CONCLUSIONS

This multiproxy investigation of the lake sediments aiming at paleoclimate and paleoenvironment reconstruction has been conducted for the first time for an unexplored taiga region located in the Central Siberian Plateau. Special attention has been paid to possible traces of the 1908 Tunguska event. The studied sediment core covers a period of about 2200 years. Our investigation has shown that, in general, the inferred climatic and limnological changes are consistent with those that occurred in the neighboring regions of Siberia and reflect the known trend of interchanging cold and warm periods in northern Eurasia. A cool and humid period occurred between 2200 and 1000 BP, though a tendency towards warming and drying had already appeared at ca. 1400 BP. A warm period corresponding to the Medieval Climatic Optimum and accompanied by a rising lake trophic status is reconstructed to have occurred between 1000 and 350 BP. An evident climate cooling corresponding to the Little Ice Age has been found to have happened after 350 BP. A trend towards climate amelioration appeared after ca. 50 BP.

Geochemical traces of the 1908 Tunguska event have been identified in the investigated core and used as a stratigraphic marker for the developed age model. No geochemical anomalies that could be associated with the extraterrestrial origin of the Tunguska event were identified. Substantial taxonomic shifts occurred in the communities of benthic chironomids and zooplankton (Cladocera) after 1908. The abundance of lotic and semi-terrestrial chironomids that survive unstable water levels or soil erosion increased. Cladoceran abundance declined almost two times, and the taxa associated with littoral vegetation disappeared. Pollen and diatom assemblages demonstrate weaker compositional shifts. Pollen concentration declined and recovered quickly. An increase in the abundance of several alkaliphile diatom species can reflect an increase in the lake's productivity. We assume this can be related to the substantial influx of terrestrial material and the rise of water turbidity from the catchment due to the tree fall and fire caused by the Tunguska event. The reaction of the biological communities of the lake and surrounding vegetation requires further investigation.

Acknowledgments. The authors thank the staff of Tungusky State Nature Reserve for their great help during the fieldwork. We would like to express our deep gratitude to Prof. Kulikovskiy MS (Institute of Inland Waters RAS, Borok) for his help in diatom identification. This study was supported by the Russian Science Foundation, Grant no. 22-17-00185 <https://rscf.ru/en/project/22-17-00185/>. Pollen analysis was carried out by N. Rudaya and Cladocera analysis was carried out by L. Frolova under the R&D Project No. FWZG-2022-0010 of the Institute of Archaeology and Ethnography SB RAS.

REFERENCES

- Abramov, N.G., Arkayev, E.A., Russkikh, A.G., 2003. The study of fire of 1908 at the area of Tunguska meteorite. In: Vasiliev, N.V., Plekhanov, G.F., Logunova L.N. et al. (Eds.), *Tunguski Natural Reserve. Proceedings 1*. [In Russian.] Tomsk State University, Tomsk, pp. 275–289.
- Agatova, A.R., Nazarov, A.N., Nepop, R.K., Rodnight, H., 2012. Holocene glacier fluctuations and climate changes in the southeastern part of the Russian Altai (South Siberia) based on a radiocarbon chronology. *Quaternary Science Reviews* 43, 74–93.
- Andreev, A., Siegert, C., Klimanov, V., Derevyagin, A., Shilova, G.N., Melles, M., 2002. Late Pleistocene and Holocene vegetation and climate on the Taymyr Lowland, Northern Siberia. *Quaternary Research* 57, 138–150.

- Baisheva, I., Biskaborn, B., Stoof-Leichenring, K., Andreev, A., Heim, B., Meucci, S., Ushnitskaya, L., et al., 2024. Late Glacial and Holocene vegetation and lake changes in SW Yakutia, Siberia, inferred from *sedaDNA*, pollen, and XRF data. *Frontiers in Earth Science*, **12**, 1354284. <https://doi.org/10.3389/feart.2024.1354284>
- Battarbee, R.W., 1986. Diatom analysis. In: Berglund, B.E. (Ed.), *Handbook of Holocene Paleolimnology and Paleohydrology*. J. Wiley & Sons, Chichester, England, pp. 527–570.
- Bennett, K.D., 1996. Determination of the number of zones in a biostratigraphical sequence. *New Phytologist* **132**, 155–170.
- Birks, H.J.B., Gordon, A.D., 1985. The analysis of pollen stratigraphical data: zonation. In: Birks, H.J.B., Gordon, A.D. (Eds.), *Numerical Methods in Quaternary Pollen Analysis*. Academic Press, London, pp. 47–90.
- Birks, H.J.B., Line, J.M., Juggins, S., Stevenson, A.C., ter Braak, C.J.F., 1990. Diatoms and pH reconstruction. *Philosophical Transactions of the Royal Society of London, Series B* **327**, 263–278.
- Biskaborn, B.K., Nazarova, L., Pestryakova, L.A., Strykh, L., Funck, K., Meyer, H., Chaplign, B., et al., 2019. Spatial distribution of environmental indicators in surface sediments of Lake Bolshoe Toko, Yakutia, Russia. *Biogeosciences* **16**, 4023–4049.
- Biskaborn, B.K., Subetto, D.A., Savelieva, L.A., Vakhrameeva, P.R., Hansche, A., Hezschuh, U., Klemm, J., et al., 2015. Late Quaternary vegetation and lake system dynamics in North-Eastern Siberia: implications for seasonal climate variability. *Quaternary Science Reviews* **147**, 406–421.
- Blyakharchuk, T.A., Wright, H.E., Borodavko, P.S., van der Knaap, W.O., Ammann, B., 2007. Late Glacial and Holocene vegetational history of the Altai Mountains (southwestern Tuva Republic, Siberia). *Palaeogeography, Palaeoclimatology, Palaeoecology* **245**, 518–534.
- Boës, X., Fagel, N., 2005. Impregnation method for detecting annual laminations in sediment cores: an overview. *Sedimentary Geology* **179**, 185–194.
- Bolobanshchikova, G.N., Rogozin, D. Yu., Firsova, A.D., Radionova, E.V., Degermendzhly, N.N., Shabanov, A.V., 2015. Analysis of diatoms in the water column and bottom sediments of Lake Shira (Khakassia, Russia). *Contemporary Problems of Ecology* **2**, 215–228.
- Brooks, S.J., Birks, H.J.B., 2001. Chironomid-inferred air temperatures from late-glacial and Holocene sites in North-West Europe: progress and problems. *Quaternary Science Reviews* **20**, 1723–1741.
- Brooks, S.J., Langdon, P.G., Heiri, O., 2007. *Using and Identifying Chironomid Larvae in Palaeoecology*. QRA Technical Guide No 10. Quaternary Research Association, London.
- Büntgen, U., Myglan, V.S., Ljungqvist, F.C., McCormick, M., Di Cosmo, N., Sigl, M., Jungclauss, J., et al., 2016. Cooling and societal change during the Late Antique Little Ice Age from 536 to around 660 AD. *Nature Geosciences* **9**, 231–236.
- Burlakov, P.S., Khmara, K.A., Belyayev, V.V., 2009. Features of the Siberian fir population *Abies sibirica* Ledeb. on the northwestern border of the range (river Ussolka, river basin of the Northern Dvina). [In Russian.] *Arctic Environmental Research* **2**, 51–57.
- Camburn, K.E., Charles, D.F., 2000. Diatoms of low-alkalinity lakes in the northeastern United States. *Academy of Natural Sciences of Philadelphia, Special Publication* **18**.
- Cao, X., Tian, F., Li, F., Gaillard, M.-J., Rudaya, N., Xu, Q., and Herzschuh, U., 2019. Pollen-based quantitative land-cover reconstruction for northern Asia covering the last 40 ka cal BP. *Climate of the Past* **15**, 1503–1536.
- Darin, A.V., Rogozin, D.Y., Meydus, A.V., Babich, V.V., Kalugin, I.A., Markovich, T.A., Rakshun, Ya. V., et al. 2020. Traces of “Tunguska 1908” event in sediments of Lake Zapovednoye according to SR-XRF data. *Doklady Earth Sciences* **492**, 442–445.
- Faegri, K., Iversen, J., 1989. *Textbook of Pollen Analysis*. John Wiley and Sons, Chichester, England.
- Farinella, P., Foschini, L., Froeschlé, C., Gonczi, R., Jopek, T.J., Longo, G., Michel, P., 2001. Probable asteroidal origin of the Tunguska Cosmic Body. *Astronomy & Astrophysics* **377**, 1081–1097.
- Fedotov, A.P., Phedorin, M.A., Enushchenko, I.V., Vershinin, K.E., Krapivina, S.M., Vologina, E.G., Petrovskii, S.K., Melgunov, M.S., Sklyarova, O.A., 2013. Drastic desalinization of small lakes in East Siberia (Russia) in the early twentieth century: inferred from sedimentological, geochemical and palynological composition of small lakes. *Environmental Earth Sciences* **68**, 1733–1744.
- Fedotov, A.P., Vorobyeva, S.S., Vershinin, K.E., Nurgaliev, D.K., Enushchenko, I.V., Krapivina, S.M., Tarakanova, K.V., Ziborova, G.A., Yassonov, P.G., Borissov, A.S., 2012. Climate changes in East Siberia (Russia) in the Holocene based on diatom, chironomid and pollen records from sediments of Lake Kotokel. *Journal of Paleolimnology* **47**, 617–630.
- Frolova, L.A., 2012. Cladocera. In: Nazarova, L.B. (Ed.), *Biological Indicators in Paleobiological Research: Atlas*. [In Russian.] Kazan University, Kazan, pp. 64–87.
- Frolova, L.A., Ibragimova, A.G., Ulrich, M., Wetterich, S., 2017. Reconstruction of the history of a thermokarst lake in the Mid-Holocene based on an analysis of subfossil Cladocera (Siberia, Central Yakutia). *Contemporary Problems of Ecology* **10**, 423–430.
- Frolova, L.A., Nigmatullin, N.M., Frolova, A.A., Nazarova, L.B., 2019. Findings of *Phreatolona protzi* (Hartwig, 1900) (Cladocera: Anomopoda: Chydoridae) in Russia. *Invertebrate Zoology* **16**, 200–210.
- Flößner, D., 2000. *Die Haplopora und Cladocera (ohne Bosminidae) Mitteleuropas*. Backhuys, Leiden.
- Gasperini, L., Alvisi, F., Biasini, G., Bonatti, E., Longo, G., Pipan, M., Ravaioli, M., Serra, R., 2007. A possible impact crater for the 1908 Tunguska Event. *Terra Nova* **19**, 245–251.
- Gavshin, V.M., Sukhorukov, F.V., Bobrov, V.A., Melgunov, M.S., Miroshnichenko, L.V., Kovalev, S.I., Romashkin, P.A., Klerkx, J., 2004. Chemical composition of uranium tail storages at Kadji-Sai (southern shore of Issyk-Kul lake, Kyrgyzstan). *Journal of Water, Air, & Soil Pollution* **154**, 71–83.
- Gladysheva, O.G., 2020. The Tunguska Event. *Ikarus* **348**, 113837. <https://doi.org/10.1016/j.ikarus.2020.113837>
- Glückler, R., Geng, R., Grimm, L., Baisheva, I., Herzschuh, U., Stoof-Leichenring, K.R., Kruse, S., Andreev, A., Pestryakova, L., Dietze, E., 2022. Holocene wildfire and vegetation dynamics in Central Yakutia, Siberia, reconstructed from lake-sediment proxies. *Frontiers in Ecology and Evolution* **10**, 962906. <https://doi.org/10.3389/fevo.2022.962906>
- Grimm, E., 2004. *Tilia Software 2.0.2*. Illinois State Museum Research and Collection Center, Springfield.
- Guiry, M.D., Guiry, G.M., 2023. AlgaeBase. World-wide electronic publication, National University of Ireland, Galway (accessed October 17, 2023). <https://www.algaebase.org>.
- Hammer, Ø., Harper, D.A.T., Raan, P.D., 2001. PAST: palaeontological statistics software package for education and data analysis. *Palaeontologia Electronica* **4**, 1–9.
- Hantemirov, R., Shiyatov, S., 2002. A continuous multi-millennial ring-width chronology in Yamal, northwestern Siberia. *The Holocene* **12**, 717–726.
- Harmsworth, R., 1968. The developmental history of Bleham Tarn (England) as shown by animal macrofossils, with special reference to the Cladocera. *Ecological Monographs* **38**, 223–241.
- Heiri, O., Brooks, S.J., Renssen, H., Bedford, A., Hazekamp, M., Ilyashuk, B., Jeffers, E.S., et al., 2014. Validation of climate model-inferred regional temperature change for late-glacial Europe. *Nature Communication* **5**, 4914. <https://doi.org/10.1038/ncomms5914>
- Heiri, O., Lotter, A.F., 2001. Effect of low count sums on quantitative environmental reconstructions: an example using subfossil chironomids. *Journal of Paleolimnology* **26**, 343–350.
- Hill, M.O., 1973. Diversity and evenness: a unifying notation and its consequences. *Ecology* **54**, 427–432.
- Hou, Q.L., Kolesnikov, E.M., Xie, L.W., Kolesnikova, N.V., Zhou, M.F. Sun, M., 2004. Platinum group element abundances in a peat layer associated with the Tunguska event, further evidence for a cosmic origin. *Planetary and Space Science* **52**, 773–773.
- Hou, Q.L., Ma, P.X., Kolesnikov, E.M., 1998. Discovery of iridium and other element anomalies near the 1908 Tunguska explosion site. *Planetary and Space Science* **46**, 163–168.
- Jenniskens, P., 2019. Tunguska eyewitness accounts, injuries and casualties. *Icarus* **327**, 4–18.
- Juggins, S., 2007. *C2 Version 1.5 User guide. Software for ecological and palaeoecological data analysis and visualisation*. Newcastle University, Newcastle upon Tyne, UK.

- Karachurina, S., Rudaya, N., Frolova, L., Kuzmina, O., Cao, X., Chepinoga, V., Stoof-Leichsenring, K., *et al.*, 2023. Terrestrial vegetation and lake aquatic community diversity under climate change during the mid-late Holocene in the Altai Mountains. *Palaeogeography, Palaeoclimatology, Palaeoecology* **623**, 111623. <https://doi.org/10.1016/j.palaeo.2023.111623>
- Khrennikov, D.E., Titov, A.K., Ershov, A.E., Pariev, V.I., Karpov, S.V., 2020. On the possibility of through passage of asteroid bodies across the Earth's atmosphere. *Monthly Notices of the Royal Astronomical Society* **493**, 1344–1351.
- Kirtman, B., Power, S.B., Adedoyin, J.A., Boer, G.J., Bojariu, R., Camilloni, I., Doblas-Reyes, F.J., *et al.*, 2013. Near-term climate change: projections and predictability. In: Stocker, T.F., Qin, D., Plattner, G.-K., Tignor, M., Allen, S.K., Boschung, J., Nauels, A., *et al.* (Eds.), *Climate Change 2013: The Physical Science Basis. Contribution of Working Group I to the Fifth Assessment Report of the Intergovernmental Panel on Climate Change*. Cambridge University Press, Cambridge, New York, pp. 953–1028.
- Klemm, J., Herzsuh, U., Pestryakova, L.A., 2015. Vegetation, climate and lake changes over the last 7000 year at the boreal tree-line in north-central Siberia. *Quaternary Science Reviews* **147**, 406–421.
- Kobe, F., Hoelzmann, P., Gliwa, J., Olschewski, P., Peskov, S.A., Shchetnikov, A.A., Danukalova, G.A., *et al.*, 2022. Lateglacial-Holocene environments and human occupation in the Upper Lena region of Eastern Siberia derived from sedimentary and zooarchaeological data from Lake Ochaul. *Quaternary International* **623**, 139–158.
- Kolesnikov, E.M., Boettger, T., Kolesnikova, N.V., 1999. Finding of probable Tunguska Cosmic Body material: isotopic anomalies of carbon and hydrogen in peat. *Planetary and Space Science* **47**, 905–916.
- Kolesnikov, E.M., Longo, G., Boettger, T., Kolesnikova, N.V., Gioacchini, P., Forlani, L., Giampieri, R., Serra, R., 2003. Isotopic-geochemical study of nitrogen and carbon in peat from the Tunguska Cosmic Body explosion site. *Icarus* **161**, 235–243.
- Kol'tsova, V.G., 1981. The history of central taiga larch forests of southern Evenkia in the Holocene. In: *Paleobotanicheskie Issledovaniya v Lesakh Severnoi Azii [Paleobotanical Investigations in Forest of Northern Asia]*. Nauka, Novosibirsk, pp. 44–62.
- Korhola, A., Rautio, M., 2001. Cladocera and other branchiopod crustaceans. In: *Tracking Environmental Change Using Lake Sediments. Vol. 4: Zoological Indicators*. Kluwer Academic Publishers, Dordrecht, pp. 125–165.
- Koshkarov, A.D., Koshkarova, V.L., 2018. Multi-century dynamics morpho-structure of forest ecosystems in Central Evenkia in a context of global climate change. [In Russian.] *Yevrasiiskii Soyuz Uchyonykh [Eurasian Union of Scientists]* **54**, 4–8.
- Koshkarova, V.I., Koshkarov, A.D., 2005. Paleocology and dynamics of forest ecosystems of Central Evenkia during the past 2400 years. *Russian Journal of Ecology* **36**, 1–7.
- Kotov, A.A., Sinev, A.Y., Glagolev, S.M., Smirnov, N.N., 2010. Water fleas (Cladocera). In: *Key Book for Zooplankton and Zoobenthos of Fresh Waters of European Russia. Vol. 1.* [In Russian.] KMK Scientific Press, Moscow pp. 151–276.
- Krammer, K., Lange-Bertalot, H., 1986. *Bacillariophyceae. Teil 1: Naviculaceae. Süßwasserflora von Mitteleuropa*. Band 2/1. VEB Gustav Fischer Verlag, Jena.
- Krammer K., Lange-Bertalot H., 1988. *Bacillariophyceae. Teil 2: Bacillariaceae, Epithemiaceae, Surirellaceae. Süßwasserflora von Mitteleuropa*. Band 2/2. VEB Gustav Fischer Verlag, Jena.
- Krammer K., Lange-Bertalot H., 1991. *Bacillariophyceae. Teil 3: Centrales, Fragilariaceae, Eunotiaceae. Süßwasserflora von Mitteleuropa*. Band 2/3. VEB Gustav Fischer Verlag, Stuttgart, Jena.
- Krishnaswami, S., Lal, D., 1978. Radionuclide limnology. In: Lerman, A. (Ed.), *Lakes: Chemistry, Geology, Physics*. Springer, Berlin, pp. 153–177.
- Krivanogov, S.K., Takahara, H., Yamamuro, M., Preis, Y.I., Khazina, I.V., Khazin, L.B., Kuzmin, Y.V., Safonova, I.Y., Ignatova, N.V., 2012. Regional to local environmental changes in southern Western Siberia: evidence from biotic records of mid to late Holocene sediments of Lake Belye. *Palaeogeography, Palaeoclimatology, Palaeoecology* **331–332**, 177–193.
- Krivanogov, S.K., Zhdanova, A.N., Solotchin, P.A., Kazansky, A.Y., Chegis, V.V., Liu, Z., Song, M., *et al.*, 2023. The Holocene environmental changes revealed from the sediments of the Yarkov sub-basin of Lake Chany, southwestern Siberia. *Geoscience Frontiers* **14**, 101518. <https://doi.org/10.1016/j.gsf.2022.101518>
- Kupriyanova, L.A., Alyoshina, L.A., 1978. *Pollen and Spores of Plants from the Flora of European Part of USSR*. Academy of Sciences USSR, Nauka, Leningrad.
- Kutafyeva, T.K., 1974. *The History of Forest Vegetation in the Interfluvium of Lower Tunguska and Podkamennaya Tunguska in Holocene*. [In Russian.] PhD thesis, Krasnoyarsk State University, Krasnoyarsk, USSR.
- Li, H.-C., Chang, Y., Berelson, W.M., Zhao, M., Misra, S., Shen, T.-T., 2022. Interannual variations of $D^{14}C_{TOC}$ and elemental contents in the laminated sediments of the Santa Barbara Basin during the past 200 years. *Frontiers in Marine Science* **9**, 823793. <https://doi.org/10.3389/fmars.2022.823793>
- Livingstone, D.M., Lotter, A.F., Walker, I.R., 1999. The decrease in summer water temperature with altitude in Swiss alpine lakes: a comparison with air lapse rates. *Arctic Antarctic and Alpine Research* **31**, 341–352.
- Longo, G., 2007. The Tunguska event. In: Bobrowsky P.T., Rickman, H. (Eds.), *Comet/Asteroid Impacts and Human Society, An Interdisciplinary Approach*. Springer-Verlag, Berlin, pp. 303–330.
- Longo, G., Serra, R., Cecchini, S., Galli, M., 1994. Search for microremnants of the Tunguska Cosmic Body. *Planetary and Space Science* **42**, 163–177.
- Lotter, A.F., Juggins, S., 1991. POLPROF, TRAN and ZONE: programs for plotting, editing and zoning pollen and diatom data. *INQUA Subcommission for the Study of the Holocene Working Group on Data-Handling Methods Newsletter* **6**, 4–6.
- Mackay, A.W., Bezrukova, E.V., Leng, M.J., Meaney, M., Nunes, A., Piotrowska, N., Self, A., *et al.*, 2012. Aquatic ecosystem responses to Holocene climate change and biome development in boreal, central Asia. *Quaternary Science Reviews* **41**, 119–131.
- Melgunov, M.S., Gavshin, V.M., Sukhorukov, F.V., Kalugin, I.A., Bobrov, V.A., Klerkx, J., 2003. Anomalies of radioactivity at the southern coast of lake Issyk-Kul (Kyrgyzstan). *Khimiya v Interesakh Ustoichivogo Razvitiya [Chemistry for Sustainable Development]* **11**, 869–880.
- Meyer, H., Chaplign, B., Hoff, U., Nazarova, L., Diekmann, B., 2015. Oxygen isotope composition of diatoms as Late Holocene climate proxy at Two-Yurts-Lake, Central Kamchatka, Russia. *Global and Planetary Change* **134**, 118–128.
- Möller Pillot, H.K.M., 2009. *Chironomidae larvae: Biology and Ecology of the Chironomini*. KNNV Publishing, Zeist, The Netherlands.
- Möller Pillot H.K.M., 2013. *Chironomidae Larvae: Biology and Ecology of the Aquatic Orthocladinae*. KNNV Publishing, Zeist, The Netherlands.
- Moore, P.D., Webb, J.A., Collison, M.E., 1991. *Pollen Analysis*. Blackwell Scientific Publications, Oxford.
- Morrison, D., 2018. *Tunguska Workshop: Applying Modern Tools to Understand the 1908 Tunguska Impact*. NASA/Technical Memorandum (NASA/TM--220174), pp. 1–15.
- Müller, S., Tarasov, P.E., Andreev, A.A., Diekmann, B., 2009. Late glacial to Holocene environments in the present-day coldest region of the Northern Hemisphere inferred from a pollen record of Lake Billyakh, Verkhoyansk Mts, NE Siberia. *Climate of the Past* **5**, 73–84.
- Naurzbaev, M.M., Vaganov, E.A., 2000. Variation of early summer and annual temperatures in east Taymyr and Putoran (Siberia) over the last two millennia inferred from tree rings. *Journal of Geophysical Research* **105**, 7317–7326.
- Naurzbaev, M.M., Vaganov, E.A., Sidorova, O.V., Schweingruber, F.H., 2002. Summer temperatures in eastern Taimyr inferred from a 2427-year late-Holocene tree-ring chronology and earlier floating series. *The Holocene* **12**, 727–736.
- Nazarova, L., Lüpfer, H., Subetto, D., Pestryakova, L., Diekmann, B., 2013. Holocene climate conditions in central Yakutia (Eastern Siberia) inferred from sediment composition and fossil chironomids of Lake Temje. *Quaternary International* **290–291**, 264–274.
- Nazarova, L., Pestryakova, L.A., Ushinckaja, L.A., Hubberten, H.-W., 2008. Chironomids (Diptera: Chironomidae) of Central Yakutian lakes and their indicative potential for palaeoclimatic investigations. *Contemporary Problems of Ecology* **1**, 335–345.
- Nazarova, L., Self, A.E., Brooks, S.J., Hardenbroek, M., Herzsuh, U., Diekmann, B., 2015. Northern Russian chironomid-based modern summer temperature data set and inference models. *Global and Planetary Change* **134**, 10–25.

- Nazarova, L.B., Self, A.E., Brooks, S.J., Solovieva, N., Syrykh, L.S., Dauvalter, V.A., 2017. Chironomid fauna of the lakes from the Pechora River basin (East of European part of Russian Arctic): ecology and reconstruction of recent ecological changes in the region. *Contemporary Problems of Ecology* **4**, 350–362.
- Nazarova, L., Syrykh, L., Grekov, I., Sapelko, T., Krasheninnikov, A.B., Solovieva, N., 2023. Chironomid-based modern summer temperature data set and inference model for the northwest European part of Russia. *Water* **15**, 976.
- Nazarova, L., Syrykh, L.S., Mayfield, R.J., Frolova, L.A., Ibragimova, A., Grekov, I.M., Subetto, D.A., 2020. Palaeoecological and palaeoclimatic conditions in Karelian Isthmus (north-western Russia) during the Holocene: multi-proxy analysis of sediments from the Lake Medvedevskoe. *Quaternary Research* **95**, 65–83.
- New, M., Lister, D., Hulme, M., Makin, I., 2002. A high-resolution data set of surface climate over global land areas. *Climate Research* **21**, 1–25.
- Palagushkina, O., Wetterich, S., Schirmermeister, L., Nazarova, L.B., 2017. Modern and fossil diatom assemblages from Bol'shoy Lyakhovsky Island (New Siberian Archipelago, Arctic Siberia). *Contemporary Problems of Ecology* **10**, 380–394.
- Patrick, R.M., Reimer, C.W., 1966. *The Diatoms of the United States Exclusive of Alaska and Hawaii*, Vol. 1. Monographs of the Academy of Natural Sciences of Philadelphia 13.
- Plikk, A., Engels, S., Luoto, T., Nazarova, L., Salonen, J. S., Helmens, K.F., 2019. Chironomid-based temperature reconstruction for the Eemian Interglacial (MIS 5e) at Sokli, northeast Finland. *Journal of Paleolimnology* **61**, 355–371.
- Pörtner, H.-O., Roberts, D.C., Tignor, M., Poloczanska, E.S., Mintenbeck, K., Alegria, A., Craig, M., et al. (Eds.), 2022. *Climate Change 2022: Impacts, Adaptation, and Vulnerability. Contribution of Working Group II to the Sixth Assessment Report of the Intergovernmental Panel on Climate Change*. Cambridge University Press, Cambridge, New York.
- Prokopenko, A.A., Khursevich, G.K., Bezrukova, E.V., Kuzmin, M.I., Boes, X., Williams, D.F., Fedenya, S.A., Kulagina, N.V., Letunova, P.P., Abzaeva, A.A., 2007. Paleoenvironmental proxy records from Lake Hovsgol, Mongolia, and a synthesis of Holocene climate change in the Lake Baikal watershed. *Quaternary Research* **68**, 2–17.
- Quinlan, R., Smol, J.P., 2001. Setting minimum head capsule abundance and taxa deletion criteria in chironomid-based inference models. *Journal of Paleolimnology* **26**, 327–342.
- R Development Core Team, 2018. *R: A Language and Environment for Statistical Computing*. R Foundation for Statistical Computing, Vienna.
- Reimer, P.J., Austin, W.E.N., Bard, E., Bayliss, A., Blackwell, P.G., Bronk Ramsey, C., Butzin, M., et al., 2020. The IntCal20 Northern Hemisphere radiocarbon calibration curve (0–55 cal kBP). *Radiocarbon* **62**, 725–757.
- Renssen, H., Seppä, H., Heiri, O., Roche, D.M., Goosse, H., Fichefet, T., 2009. The spatial and temporal complexity of the Holocene thermal maximum. *Nature Geoscience* **2**, 410–413.
- Rogozin, D.Y., Darin, A.V., Kalugin, I.A., Melgunov, M.C., Meydus, A.V., Degermendzhi, A.G., 2017. Sedimentation rate in Lake Cheko (Evenkia, Siberia): new evidence to the problem of 1908 Tunguska Event. *Doklady Earth Sciences* **476**, 1226–1228.
- Rogozin, D.Y., Krylov, P.S., Dautov, A.N., Darin, A.V., Kalugin, I.A., Meydus, A.V., Degermendzhi, A.G., 2023. Morphology of lakes of the Central Tunguska Plateau (Krasnoyarsk krai, Evenkia): new data on the problem of the Tunguska Event of 1908. *Doklady Earth Sciences* **510**, 307–311.
- Rudaya, N., Krivonogov, S., Słowinski, M., Cao, X., Zhilich, S., 2020. Postglacial history of the Steppe Altai: climate, fire and plant diversity. *Quaternary Science Reviews* **249**, 106616. <https://doi.org/10.1016/j.quascirev.2020.106616>
- Rudaya, N., Nazarova, L., Nourgaliev, D., Palagushkina, O., Papin, D., Frolova, L., 2012. Middle-Late Holocene environmental history of Kulunda, southwestern Siberia: vegetation, climate and humans. *Quaternary Science Reviews* **48**, 32–42.
- Rudaya, N., Nazarova, L., Novenko, E., Andreev, A., Babich, V., Kalugin, I., Daryin, A., Li, H.-Ch., Shilov, P., 2016. Quantitative reconstructions of mid-late Holocene climate and vegetation in the north-eastern Altai Mountains recorded in Lake Teletskoye. *Global and Planetary Change* **141**, 12–24.
- Rudoy, A.N., Lysenkova, Z.V., Rudski, V.V., Shishin, M. Yu., 2000. *Ukok*. [In Russian.] Altai University Press, Barnaul.
- Self, A.E., Jones, V.J., Brooks, S.J., 2015. Late Holocene environmental change in arctic western Siberia. *The Holocene* **25**, 150–165.
- Shumilova, L.V., 1962. *Botanical Geography of Siberia*. [In Russian.] Tomsk State University, Tomsk.
- Smirnov, N.N., 1971. *Chydoridae (Chydoridae fauny mira)*. Fauna of the U.S.S.R. Vol. 1. Nauka, Leningrad.
- Solomina, O.N., 1999. *Gornoe Oledenenie Severnoi Evrasii v Golotsene [Mountain Glaciation of Northern Eurasia in the Holocene]*. Nauchnyi mir, Moscow.
- Sorrel, P., Jacq, K., Van Exem, A., Escarguel, G., Dietred, B., Debret, M., McGowan, S., Ducept, J., Gauthier, E., Oberhänsli, H., 2021. Evidence for centennial-scale Mid-Holocene episodes of hypolimnetic anoxia in a high-altitude lake system from central Tian Shan (Kyrgyzstan). *Quaternary Science Reviews* **252**, 106748. <https://doi.org/10.1016/j.quascirev.2020.106748>
- Stenina, A.S., 2009. *Diatom Algae (Bacillariophyta) in the Lakes of the East of Bolshezemel'skaya Tundra*. [In Russian.] Institute of Biology of Komi Scientific Center, Syktyvkar.
- Stine, S., 1998. Medieval climatic anomaly in the Americas. In: Issar, A.S., Brown, N. (Eds.), *Water, Environment and Society in Times of Climatic Change*. Kluwer, Dordrecht, pp. 43–67.
- Stockmarr, J., 1971. Tablets with spores used in absolute pollen analysis. *Pollen et Spores* **13**, 615–621.
- Subetto, D.A., Nazarova, L.B., Pestryakova, L.A., Syrykh, L.S., Andronikov, A.V., Biskaborn, B., Diekmann, B., Kuznetsov, D.D., Sapelko, T.V., Grekov, I.M., 2017. Palaeolimnological studies in Russian Northern Eurasia: a review. *Contemporary Problems of Ecology* **4**, 327–335.
- Syrykh, L.S., Nazarova, L.B., Herzsuh, U., Subetto, D.A., Grekov, I.M., 2017. Reconstruction of palaeoecological and palaeoclimatic conditions of the Holocene in the south of Taimyr according to the analysis of lake sediments. *Contemporary Problems of Ecology* **4**, 363–369.
- Szeroczyńska, K., Sarmaja-Korjonen, K., 2007. *Atlas of Subfossil Cladocera from Central and Northern Europe*. Friends of the Lower Vistula Society, Świecie.
- ter Braak, C.J.F., Prentice, I.C., 1988. A theory of gradient analysis. *Advances in Ecological Research* **18**, 271–317.
- ter Braak, C.J.F., Šmilauer, P., 2002. *CANOCO for Windows: Software for Community Ordination Version 4.5*. Microcomputer Power, Ithaca, New York.
- Trifonova, I.S., 1990. *Ecology and Succession of Lacustrine Plankton*. [In Russian.] Leningrad, Nauka.
- Vasiliev, N.V., Lvov, Y.A., 2003. Program of scientific research in Tunguski Natural Reserve 2000–2003. In: Vasiliev, N.V., Plekhanov, G.F., Logunova, L.N., Boyarko, E.Y., Ivanova, G.M., Muldiyarov, E.Y. (Eds.), *Tunguski Natural Reserve. Proceedings 1*. [In Russian.] Tomsk State University, Tomsk, pp. 14–33.
- Vasiliev, N.V., Lvov, Y.A., Plekhanov, G.F., Logunova, L.N., Muldiyarov, E.Y., Bibikova, V.V., Volkov, A.E., et al., 2003. Tunguski Natural Reserve (basic data outline). In: Vasiliev, N.V., Plekhanov, G.F., Logunova, L.N., Boyarko, E.Y., Ivanova, G.M., Muldiyarov, E.Y. (Eds.), *Tunguski Natural Reserve. Proceedings 1*. [In Russian.] Tomsk State University, Tomsk, pp. 33–90.
- Vegas-Vilarrúbia, T., Corella, J.P., Pérez-Zanón, N., Buchaca, T., Trapote, M.C., López, P., Sigró, J., Valentí Rull, V., 2018. Historical shifts in oxygenation regime as recorded in the laminated sediments of lake Montcortès (Central Pyrenees) support hypoxia as a continental-scale phenomenon. *Science of The Total Environment* **612**, 1577–1592.
- Walker, M.J.C., 2006. *Quaternary Dating Methods*. John Wiley & Sons, Chichester, England.
- Watchorn, M.A., Hamilton, P.B., Anderson, T.W., Roe, H.M., Patterson, R.T., 2008. Diatoms and pollen as indicators of water quality and land-use change: a case study from the Oak Ridges Moraine, Southern Ontario, Canada. *Journal of Paleolimnology* **39**, 491–509.

- Wetterich, S., Rudaya, N., Nazarova, L., Syrykh, L., Pavlova, M., Palagushkina, O., Kizyakov, A., *et al.*, 2021. Paleo-ecology of the Yedoma Ice Complex on Sobo-Sise Island (Eastern Lena Delta, North-east Siberian Arctic). *Frontiers in Earth Science* **9**, 681511. <https://doi.org/10.3389/feart.2021.681511>
- Wetterich, S., Schirrmeister, L., Nazarova, L., 2018. Holocene thermokarst and pingo development in the Kolyma Lowland 1 (NE Siberia). *Permafrost and Periglacial Processes* **29**, 182–198.
- Whipple, F.J.W., 1934. On phenomena related to the great Siberian meteor. *Quarterly Journal of the Royal Meteorological Society* **60**, 505–522.
- Wiederholm, T., 1983. *Chironomidae of the Holarctic Region: Keys and Diagnoses. Part 1: Larvae*. Entomologica Scandinavica 19.
- Wirth, S.B., Gilli, A., Niemann, H., Dahl, T.W., Ravasi, D., Sax, N., Hamann, Y., *et al.*, 2013. Combining sedimentological, trace metal (Mn, Mo) and molecular evidence for reconstructing past water-column redox conditions: the example of meromictic Lake Cadagno (Swiss Alps). *Geochimica et Cosmochimica Acta* **120**, 220–238.
- Zeeberg, J., Forman, S.L., Polyak, L., 2003. Glacier extent in a Novaya Zemlya fjord during the 'Little Ice Age' inferred from glaciomarine sediment records. *Polar Research* **22**, 385–394.
- Zhen, Z.L., Li, W.B., Xu, L.S., Wang, C.L., Zhao, L.T., 2020. Characteristics of palaeosalinity and palaeoredox records in sediment from Dali Lake: climate change in North China from 0 to 2100 cal BP. *Quaternary Geochronology* **60**, 101104.
- Zhilich S., Rudaya, N., Krivonogov, S., Nazarova, L., Pozdnyakov, D., 2017. Environmental dynamics of the Baraba forest-steppe over the last 8000 years and their impact on the types of economic life of the population. *Quaternary Science Reviews* **163**, 152–161.